RESEARCH MEMORANDUM

PRESSURE DISTRIBUTIONS OVER A RETRACTED LEADING-EDGE SLAT ON A 40° SWEPTBACK WING AT MACH NUMBERS UP TO 0.9

By Jones F. Cahill and Gale C. Oberndorfer

Langley Aeronautical Laboratory
Langley Field, Va.

NATIONAL ADVISORY COMMITTEE
FOR AERONAUTICS

WASHINGTON
January 26, 1951

NATIONAL ADVISORY COMMITTEE FOR AERONAUTICS

RESEARCH MEMORANDUM

PRESSURE DISTRIBUTIONS OVER A RETRACTED LEADING-EDGE SLAT ON A 40° SWEPTBACK WING AT MACH NUMBERS UP TO 0.9

By Jones F. Cahill and Gale C. Oberndorfer

SUMMARY

Pressure distributions over a retracted leading-edge slat on a 40° sweptback wing are presented for a series of angles of attack up to maximum lift at Mach numbers of 0.1, 0.4, 0.6, 0.7, 0.8, 0.85, and 0.9. These data were obtained in the Langley low-turbulence pressure tunnel at a constant Reynolds number of approximately 3×10^6. The Reynolds number was maintained approximately constant through the Mach number range by varying the stagnation pressure.

INTRODUCTION

As the first phase of an investigation of leading-edge slat loads for sweptback wings at high subsonic speeds, tests have been made in the Langley low-turbulence pressure tunnel to determine the pressure distribution around the leading edge of a 40° sweptback wing at Mach numbers up to 0.9.

In order to make these data available immediately, the pressure-distribution data obtained at a representative series of angles of attack are presented herein with no analysis or discussion. These pressure-distribution data may be used to predict the loads on leading-edge slats of various sizes (up to 0.25-wing chord) in the retracted condition. The remaining phase of this investigation will include the determination of the loads on an extended leading-edge slat on the same wing through a range of subsonic Mach numbers.

SYMBOLS

α	angle of attack
C_L	lift coefficient $\left(\frac{L}{qS_w}\right)$
L	lift on semispan wing
S_w	area of semispan wing
q	stream dynamic pressure
S	pressure coefficient $\left(\frac{H_o - p}{q}\right)$
H_o	stream stagnation pressure
p	local static pressure
M	Mach number
x	chordwise location
y	spanwise location
z	orifice location perpendicular to chord line
c	wing chord perpendicular to leading edge
$c^*/4$	quarter chord of unswept wing panel
c_s	chord of hypothetical slat, 0.22c
$b/2$	wing semispan

Description of Model and Tests

The model used in these tests is the same model used for the investigation reported in reference 1. A sketch of the model is shown in figure 1. The wing sweep, defined as the sweep angle of the quarter-chord line of an equivalent unswept wing, was 40°. This quarter-chord line becomes the 0.273-chord line of the swept wing measured parallel to the plane of symmetry. The wing was composed of NACA 64_1-112 airfoil sections perpendicular to the 0.273-chord line. The wing had no geometrical twist or dihedral, an aspect ratio of 4, and a taper ratio of 0.625.

Orifices were installed in the wing at five spanwise stations, in lines perpendicular to the wing leading edge. The location of these orifices is shown in figure 1(b). The orifices at each spanwise station extended from 0.05c on the lower surface around the leading edge to 0.25c on the upper surface. The orifices were connected to a multiple-tube manometer and pressures were recorded photographically.

The model was mounted on an electric resistance-type strain-gage semispan balance. Lift and pressure-distribution data were recorded for a range of angle of attack from zero lift to about maximum lift for Mach numbers of 0.1, 0.4, 0.6, 0.7, 0.8, 0.85, and 0.9 for the wing alone and at a Mach number of 0.1 for the wing with a half-span trailing-edge split flap having a chord equal to 18.4 percent of the wing chord parallel to the plane of symmetry and deflected 60° about its hinge line. All tests were made at a Reynolds number of approximately 3×10^6. Jet-boundary corrections to the angle of attack were applied by using the method described in reference 2. No blocking corrections were applied to the data presented in this paper. The jet blocking corrections were calculated at a number of conditions and were found to have a maximum value of about 2 percent at maximum lift at the highest Mach numbers.

The tests at a Mach number of 0.1 were made in air while all those at higher Mach numbers were made in an atmosphere of Freon-12. Conversion factors have been applied to the data measured in Freon-12 to convert them to corresponding air data.

Presentation and Application of Data

Lift characteristics of the wing are presented in figure 2. Pressure-distribution data for a series of angles of attack at Mach numbers of 0.1, 0.4, 0.6, 0.7, 0.8, 0.85, and 0.9 are shown in figures 3 to 10. The pressure coefficients are plotted against the chordwise position of the orifices, defined in terms of the chord of a hypothetical leading-edge slat having a chord of 22 percent of the wing chord perpendicular to the wing leading edge.

Normal forces or chord forces on a leading-edge slat of any size, up to 25 percent of the wing chord, may be obtained from the pressure-distribution data presented by integrating the pressures with respect to the orifice locations parallel or perpendicular to the chord, respectively. The pressures on the lower surface of the slat may have any value between the pressure at the wing-slat juncture on the lower surface

and that on the upper surface, depending upon the manner in which the juncture is sealed.

Langley Aeronautical Laboratory
National Advisory Committee for Aeronautics
Langley Field, Va.

REFERENCES

1. Cahill, Jones F.: Comparison of Semispan Data Obtained in the Langley Two-Dimensional Low-Turbulence Pressure Tunnel and Full-Span Data Obtained in the Langley 19-Foot Pressure Tunnel for a Wing with 40° Sweepback of the 0.27-Chord Line. NACA RM L9B25a, 1949.

2. Katzoff, S., and Hannah, Margery E.: Calculation of Tunnel-Induced Upwash Velocities for Swept and Yawed Wings. NACA TN 1748, 1948.

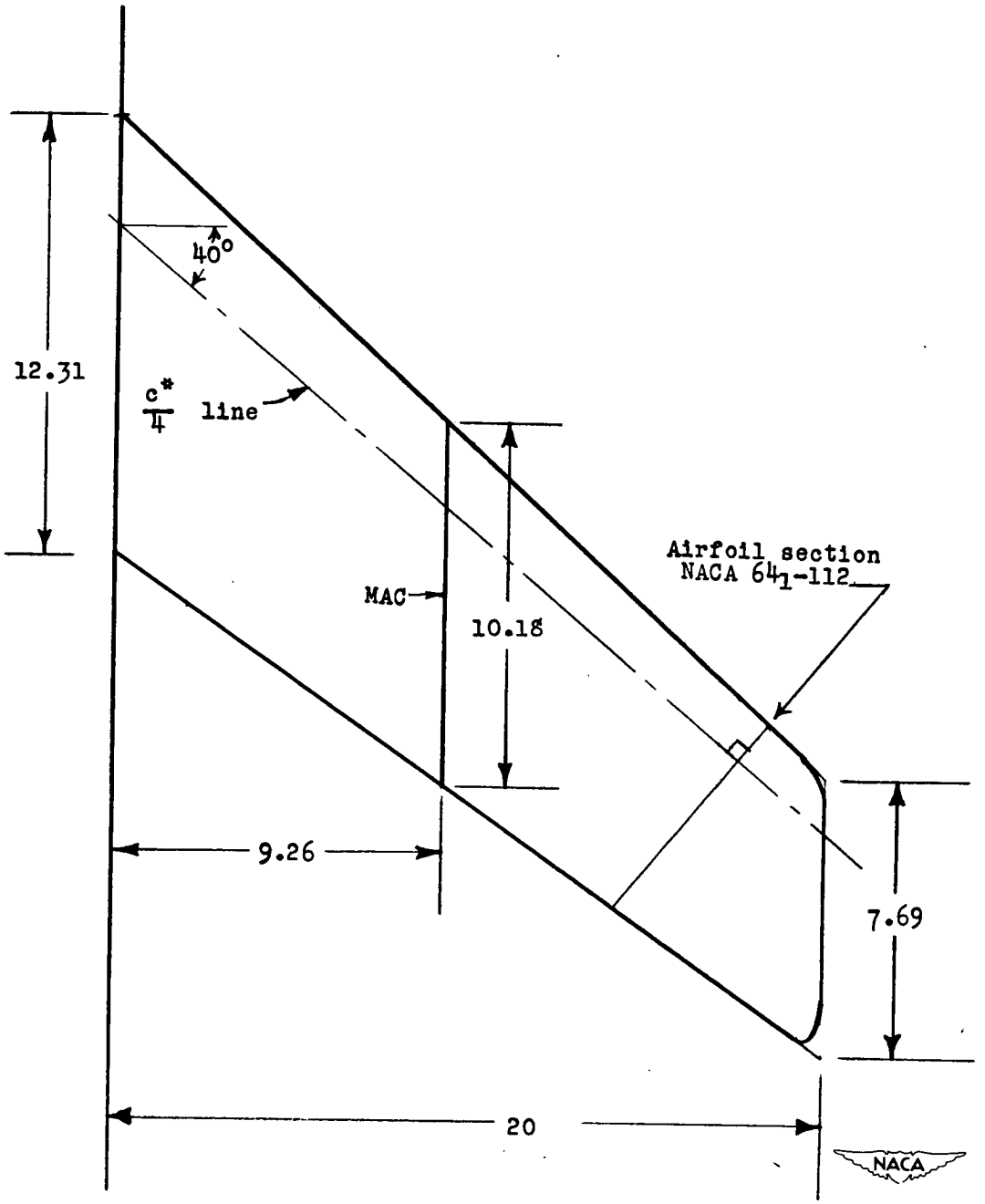

(a) Plan form of basic wing.

Figure 1.- Sketch of 40° sweptback wing.
All dimensions given in inches.

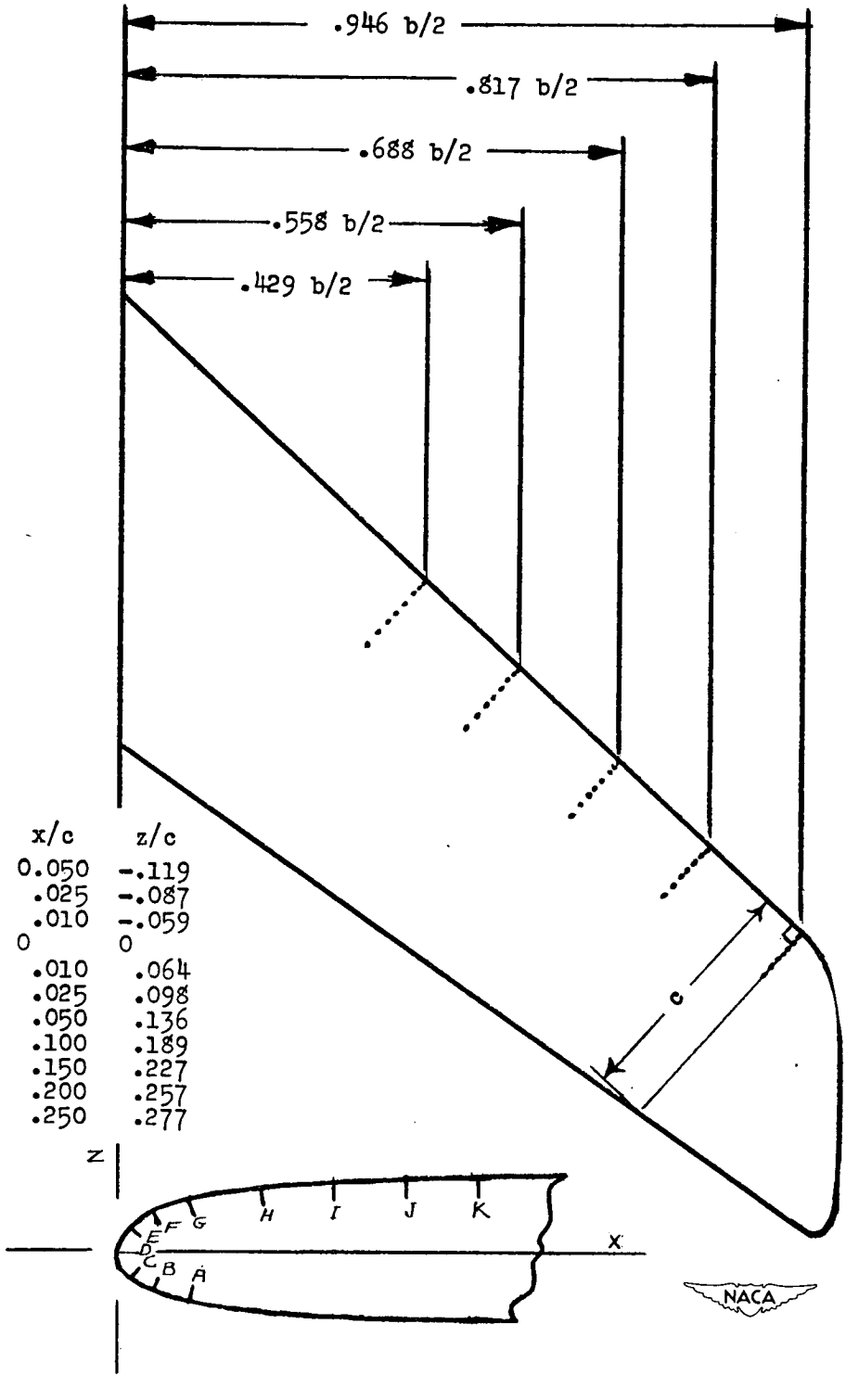

Orifice	x/c	z/c
A	0.050	-.119
B	.025	-.087
C	.010	-.059
D	0	0
E	.010	.064
F	.025	.098
G	.050	.136
H	.100	.189
I	.150	.227
J	.200	.257
K	.250	.277

(b) Orifice locations

Figure 1.- Concluded

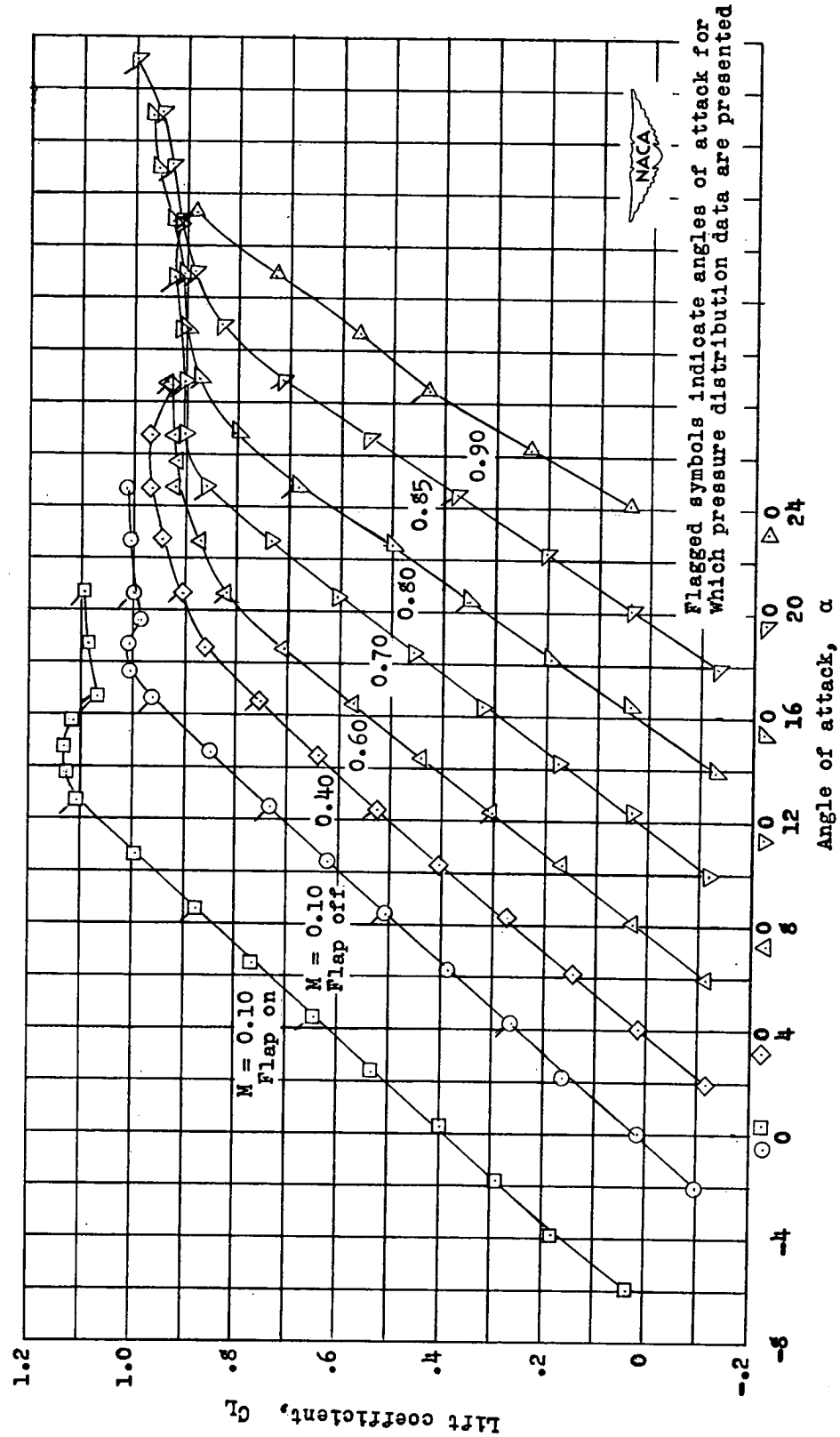

Figure 2.- Lift characteristics of wing at various Mach numbers.

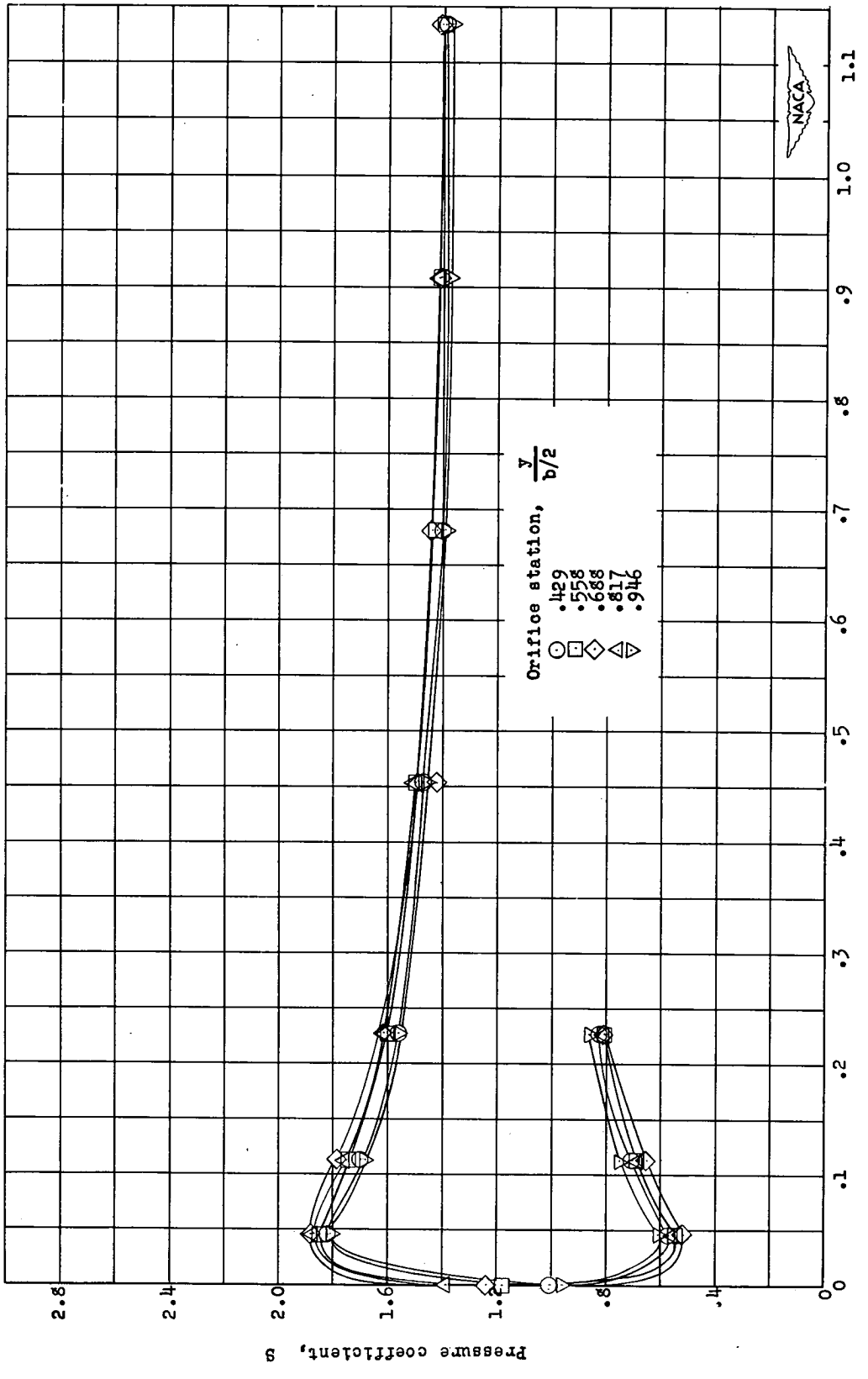

(a) $\alpha = 4.2°$.

Figure 3.- Pressure distribution about wing leading edge at various angles of attack. M = 0.10. Flap off.

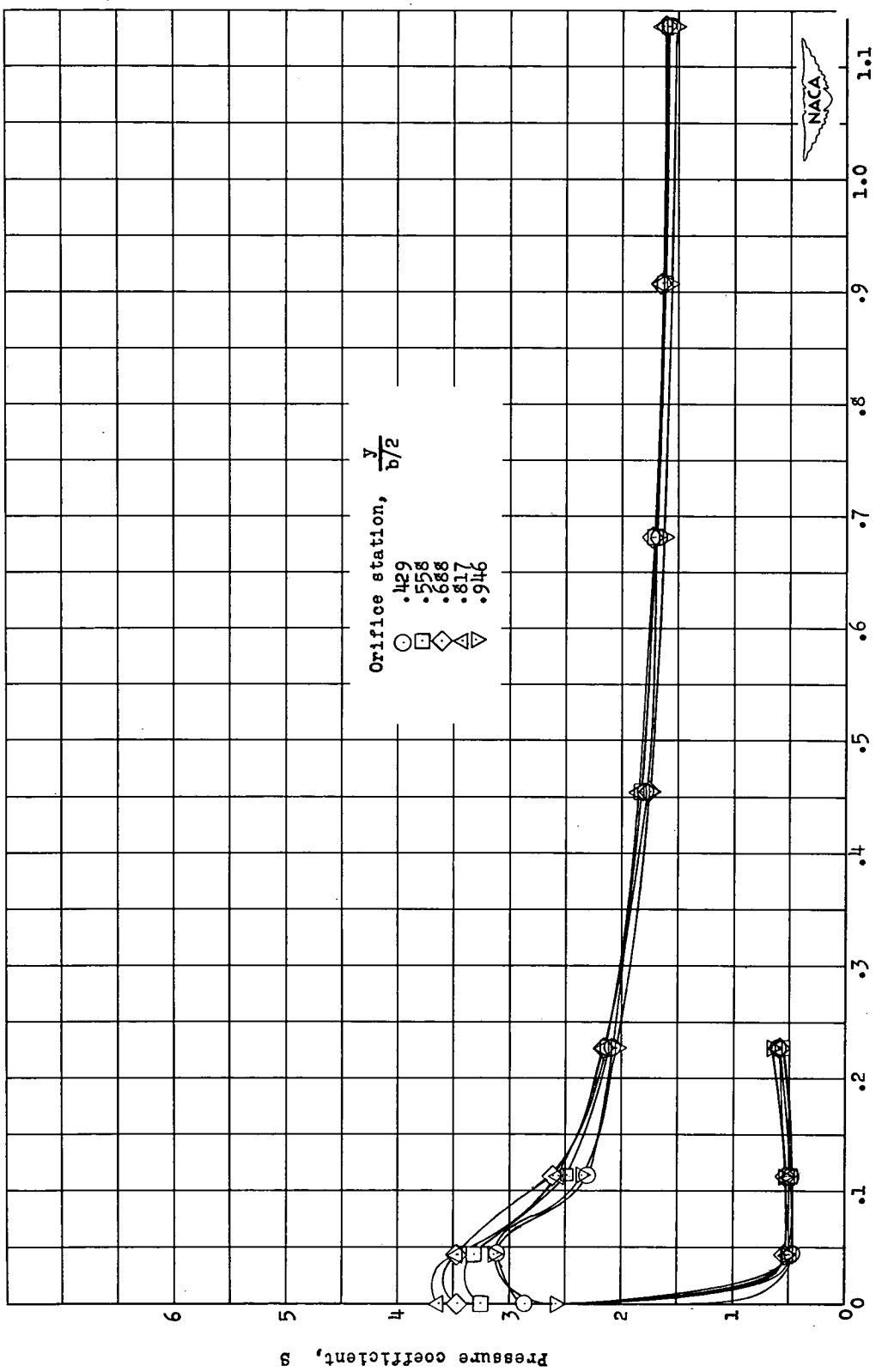

(b) $\alpha = 8.3°$.

Figure 3.- Continued

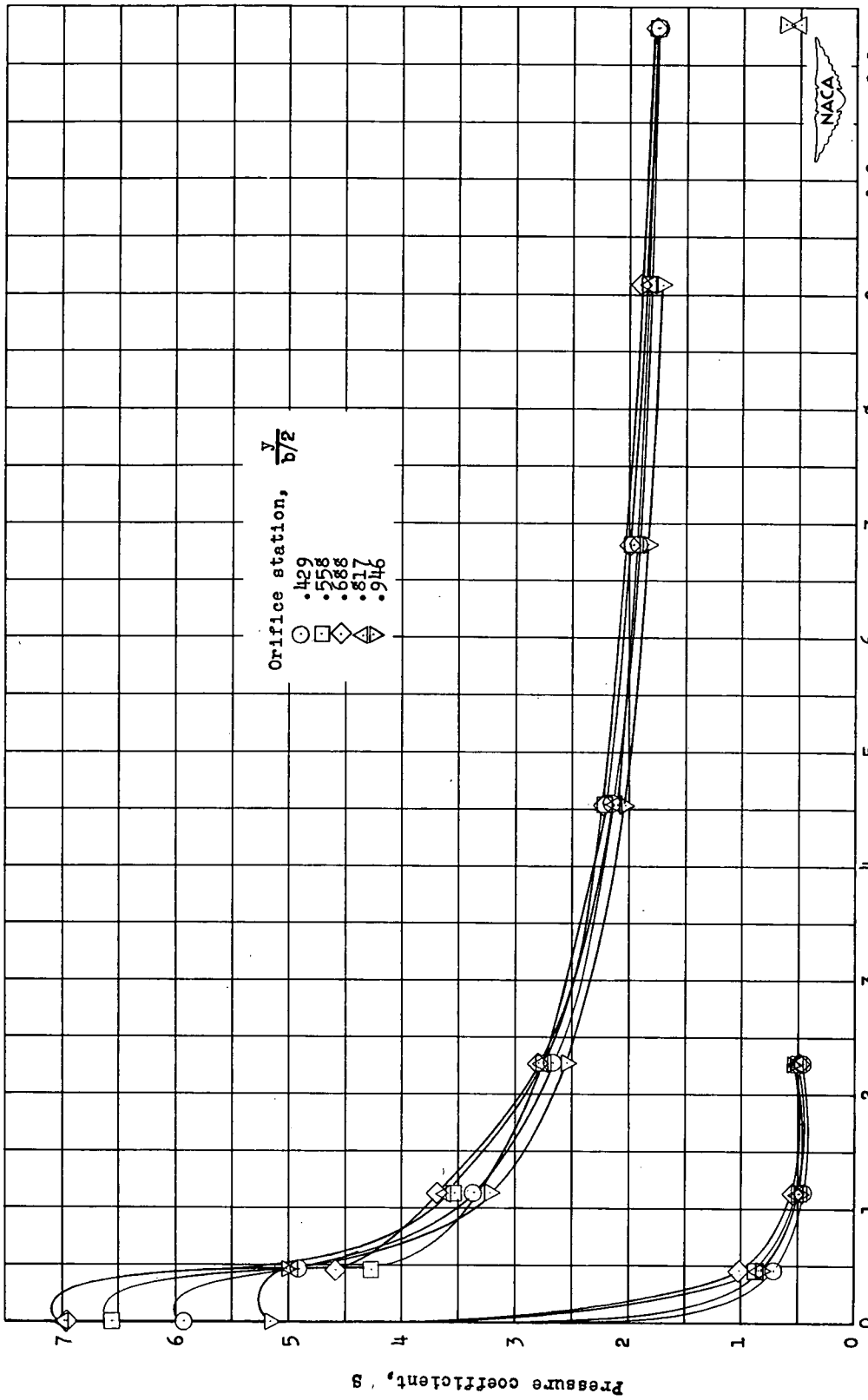

(c) $\alpha = 12.4°$.

Figure 3.- Continued

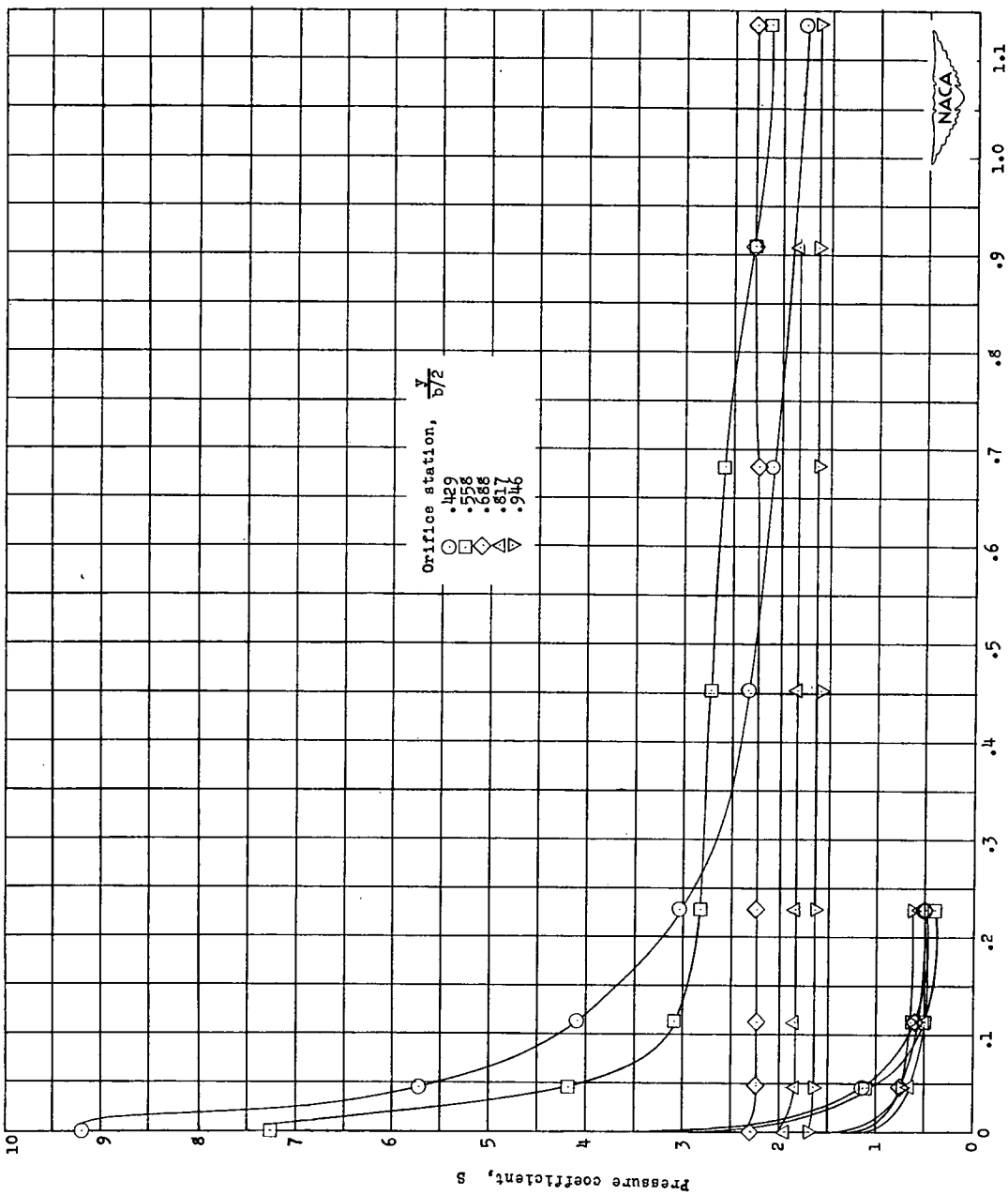

(d) $\alpha = 16.6°$.

Figure 3.- Continued

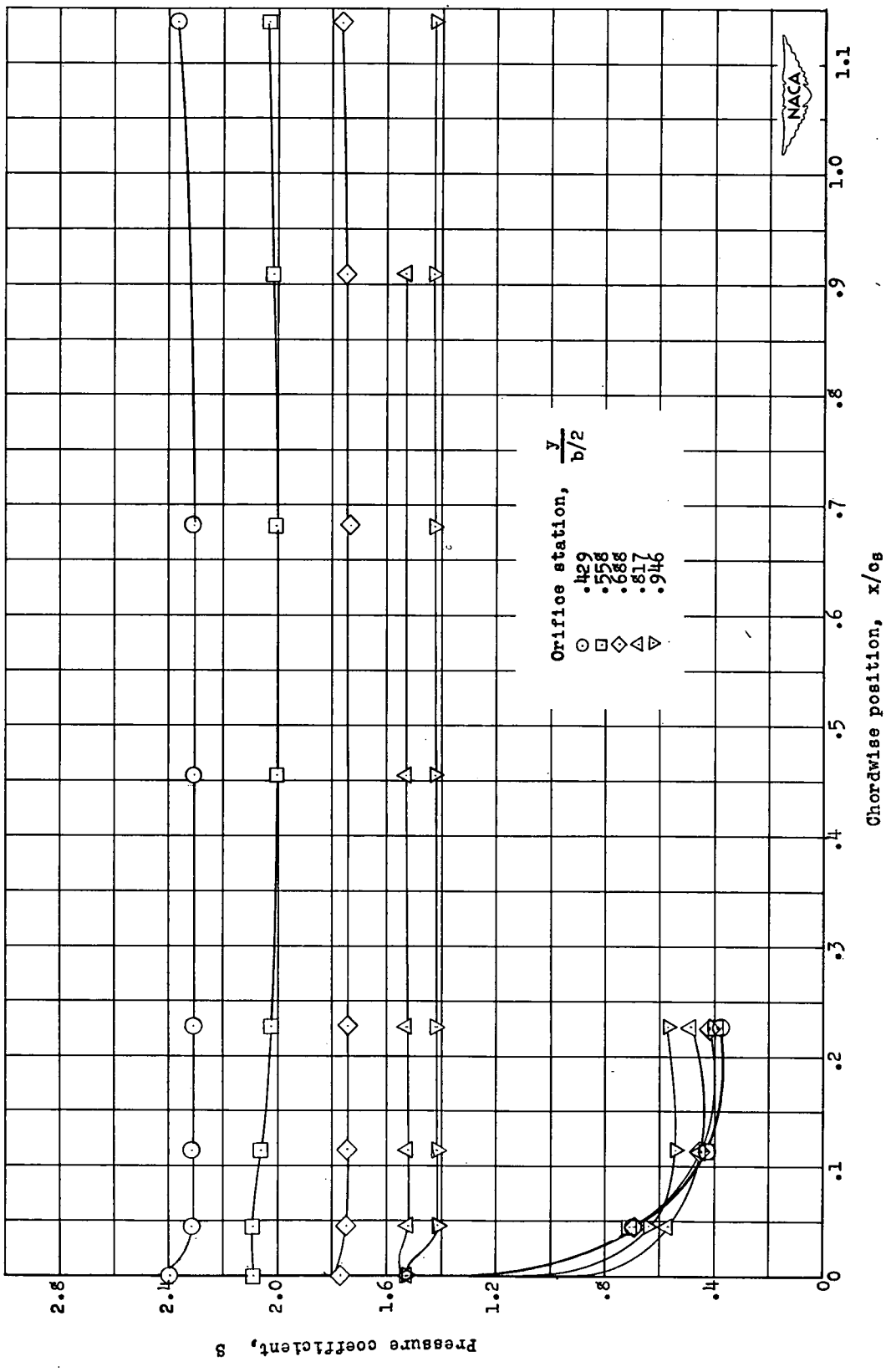

(e) $\alpha = 20.6°$.

Figure 3.- Concluded.

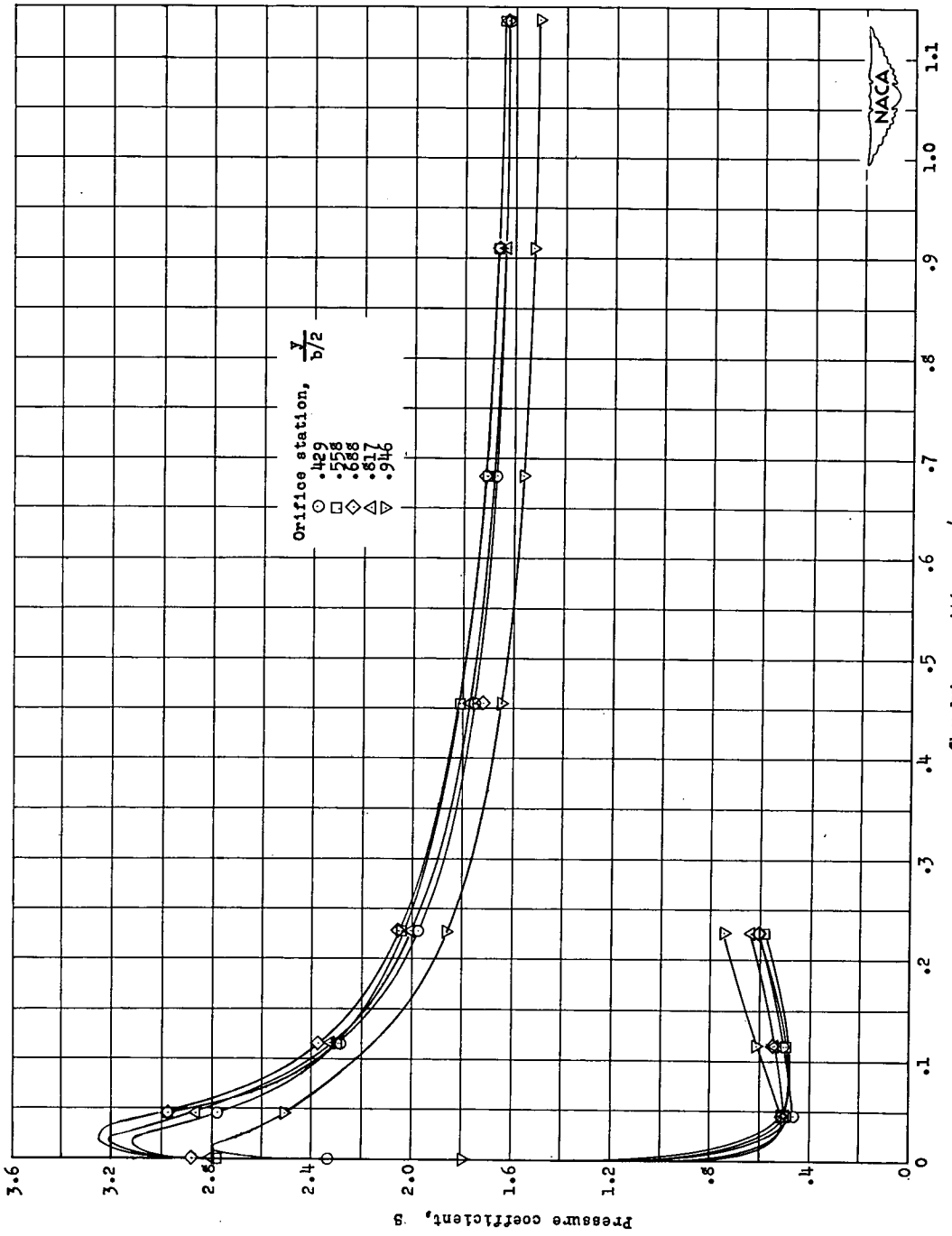

(a) $\alpha = 4.4^{\circ}$.

Figure 4.- Pressure distribution about wing leading edge at various angles of attack. M = 0.10. Flap on.

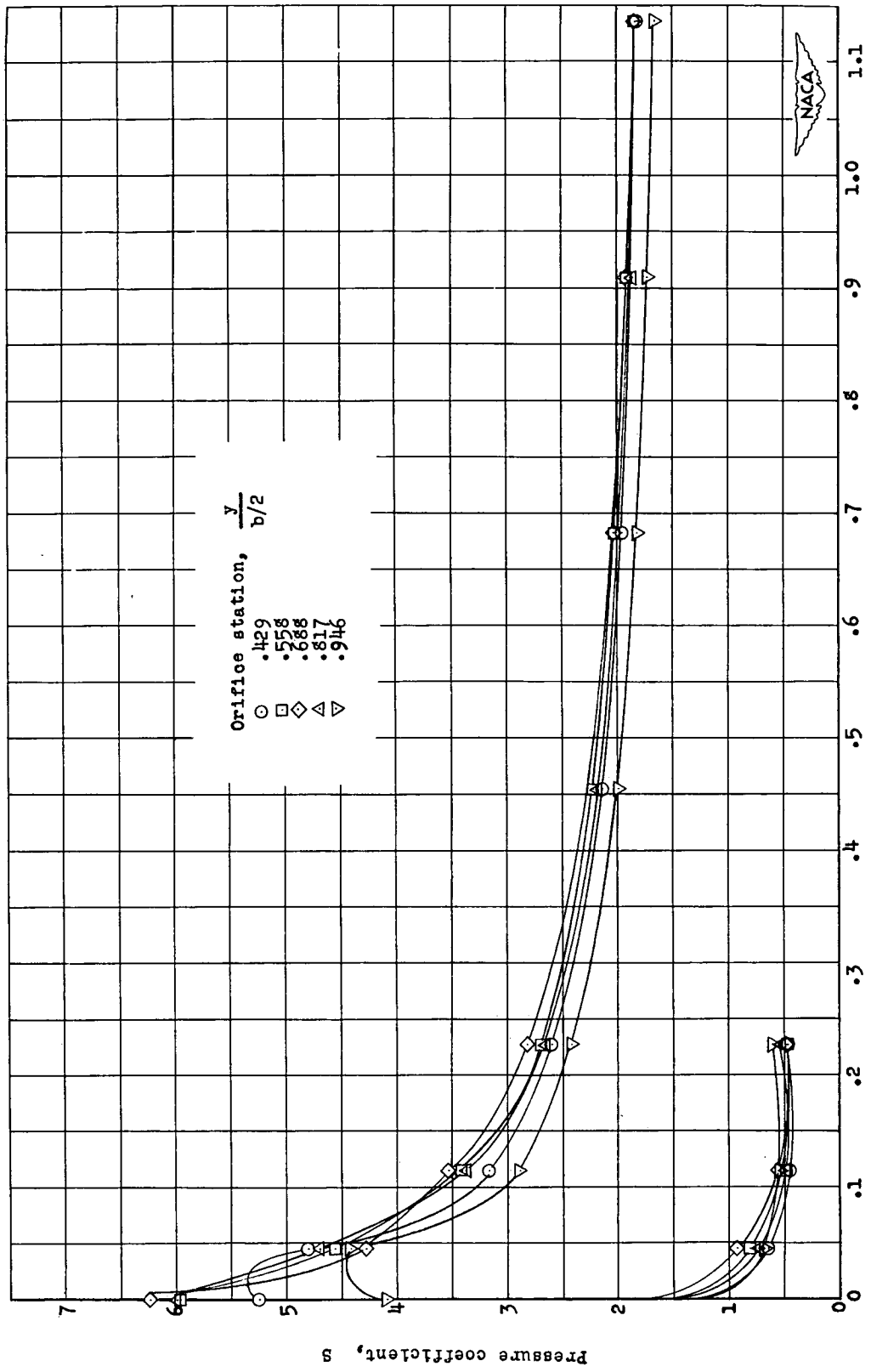

(b) $\alpha = 8.5°$.

Figure 4.- Continued.

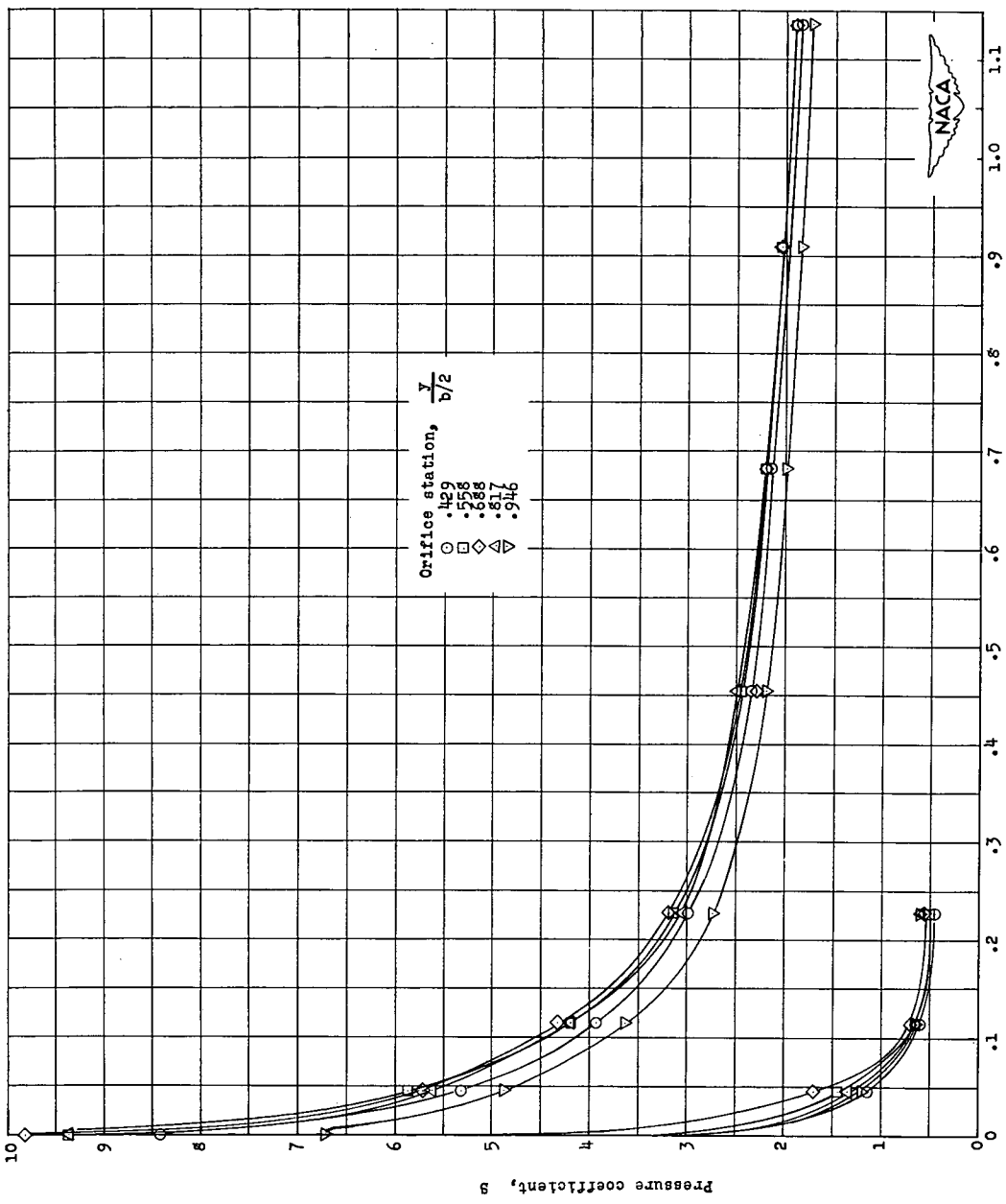

(c) $\alpha = 12.7°$.

Figure 4.- Continued.

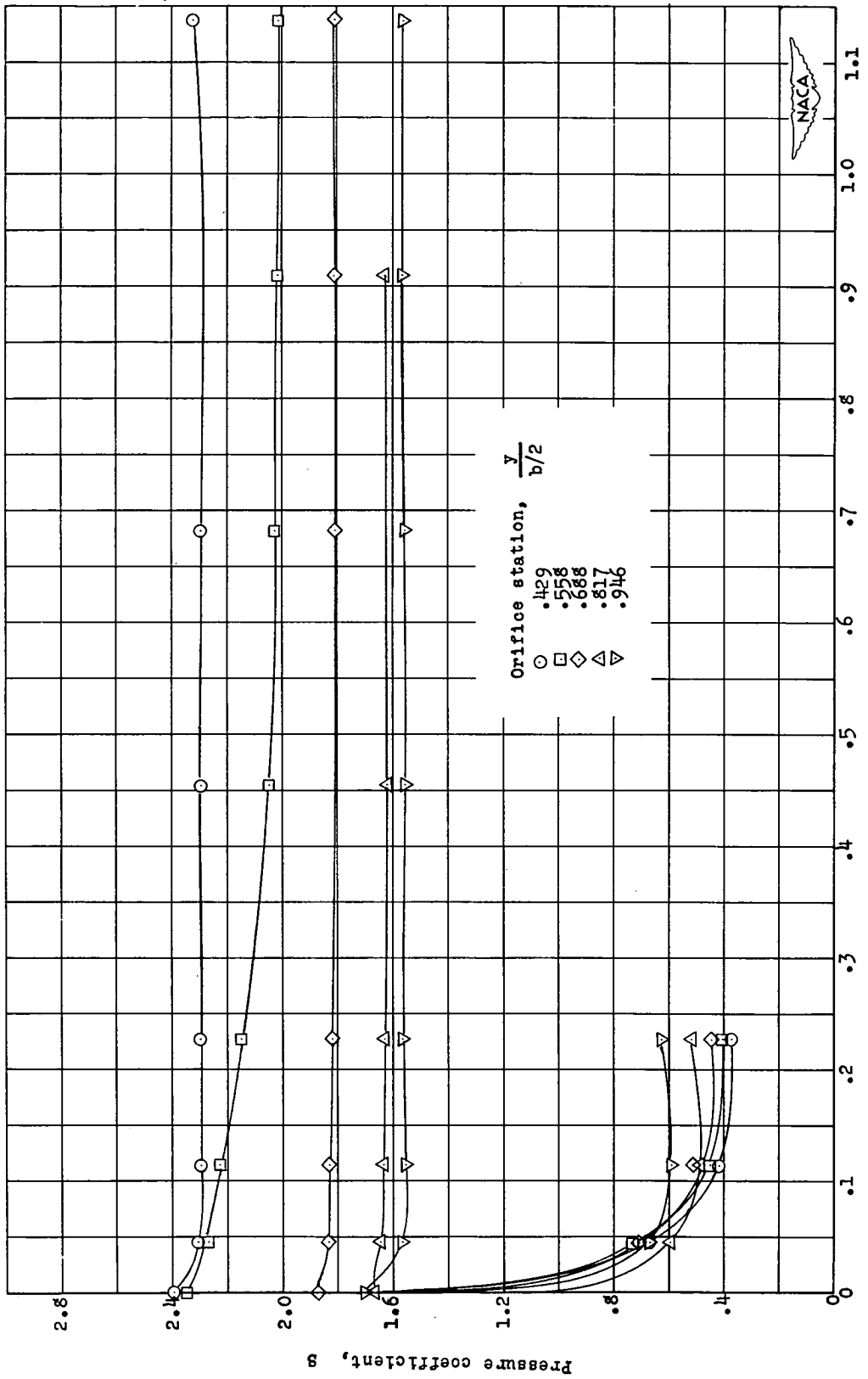

(d) $\alpha = 16.6°$.

Figure 4.- Continued.

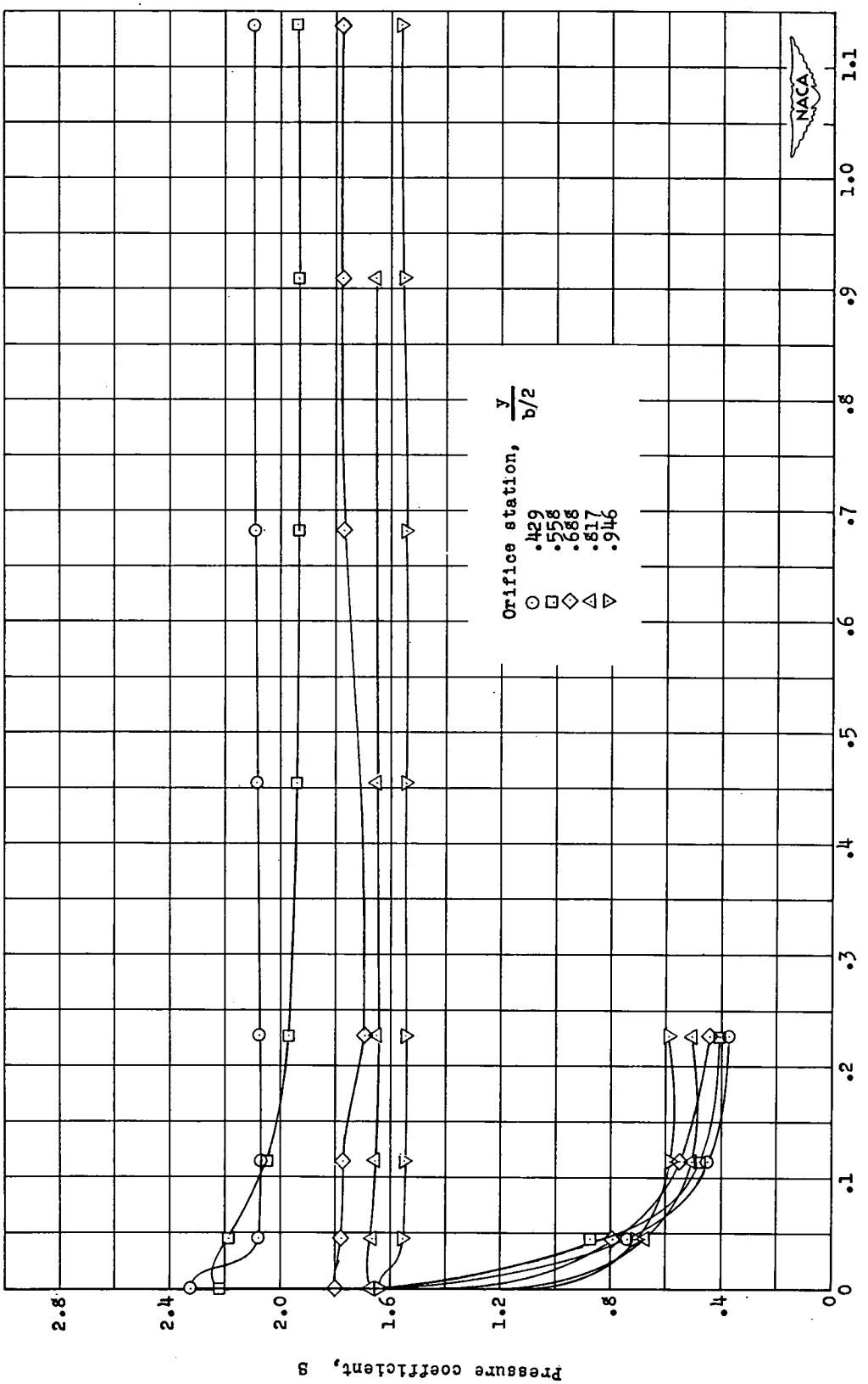

(e) $\alpha = 20.7^{\circ}$.

Figure 4.- Concluded

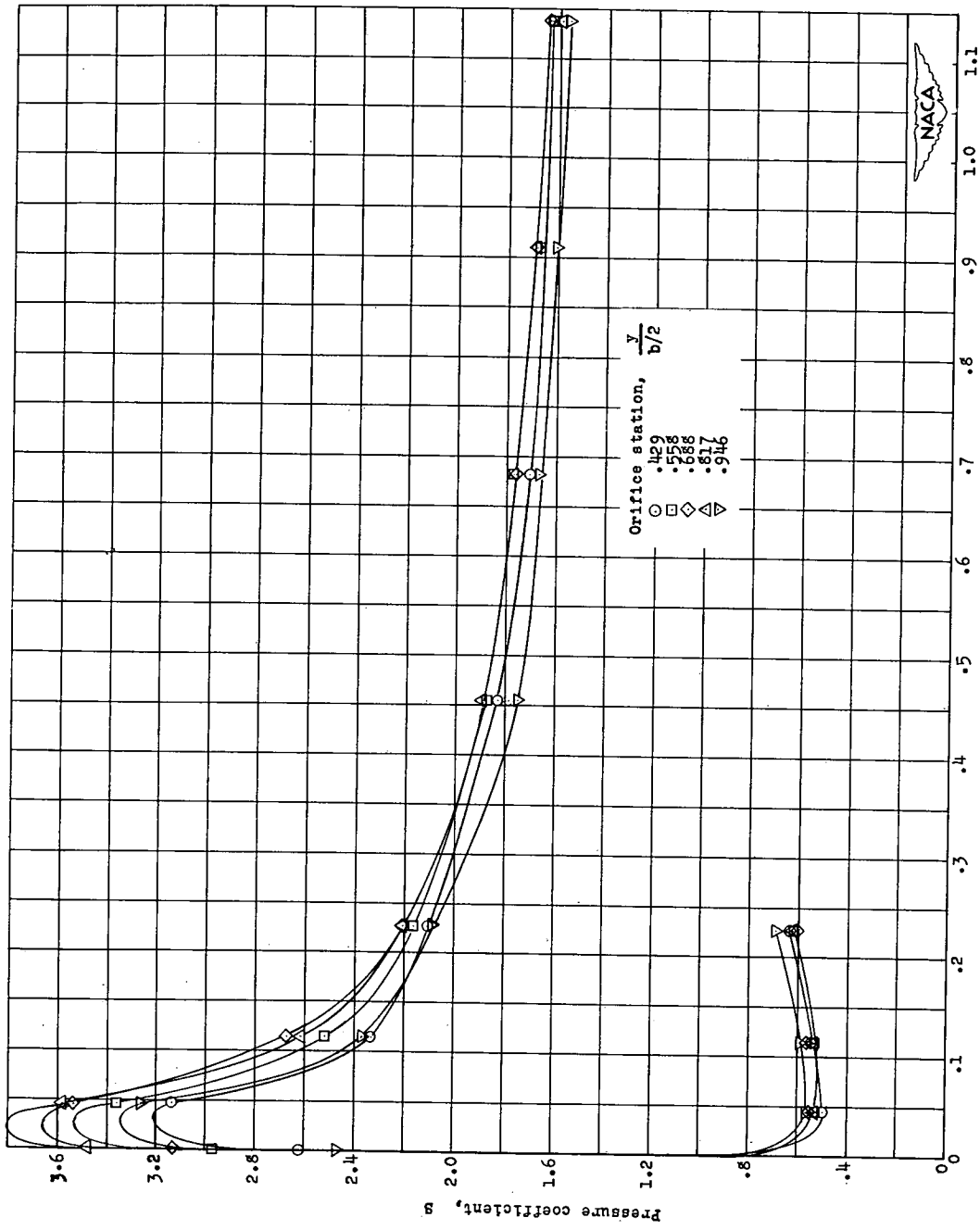

(a) $\alpha = 8.4^{\circ}$.

Figure 5.- Pressure distribution about wing leading edge at various angles of attack. M = 0.40. Flap off.

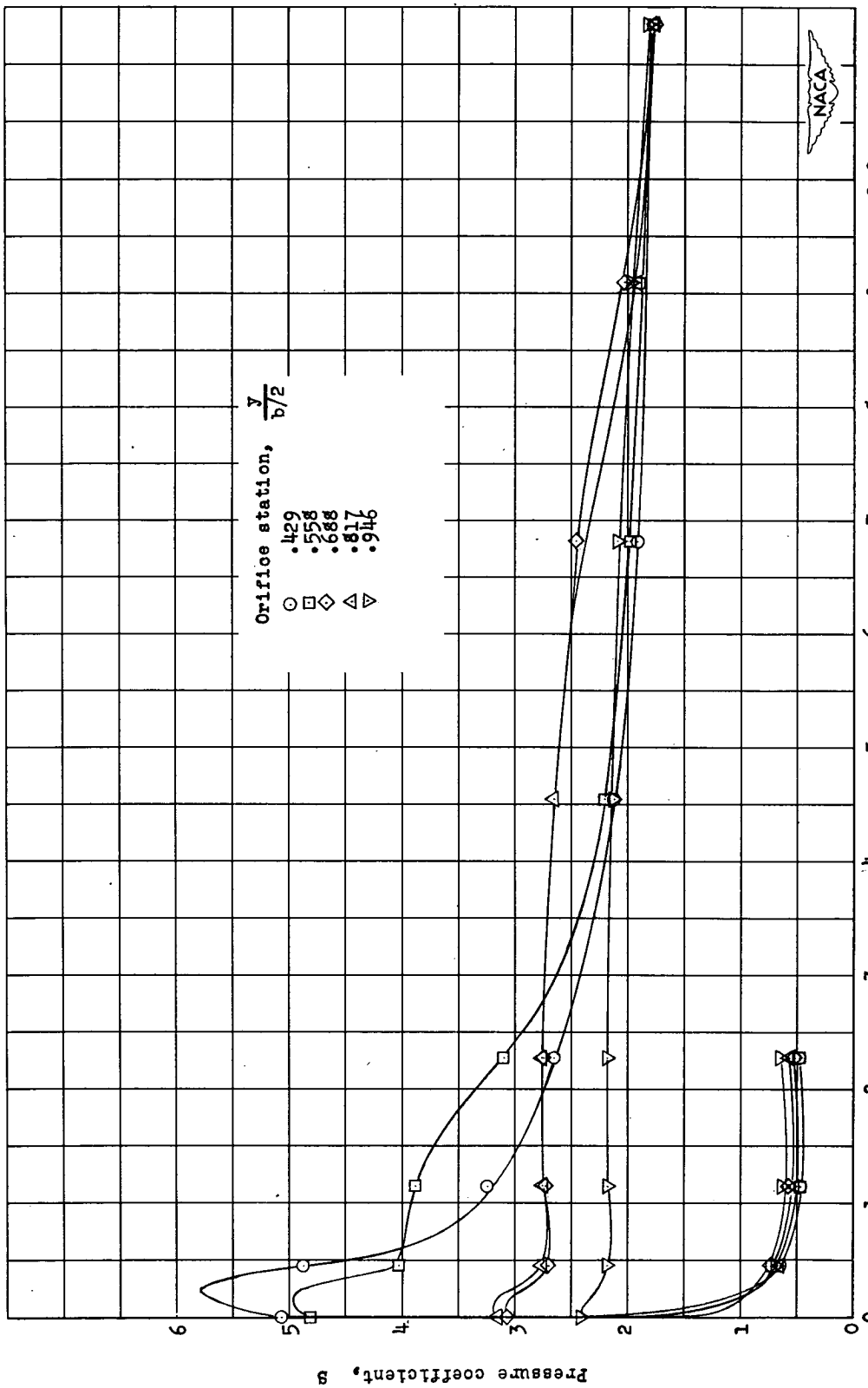

(b) $\alpha = 12.5°$.

Figure 5.- Continued.

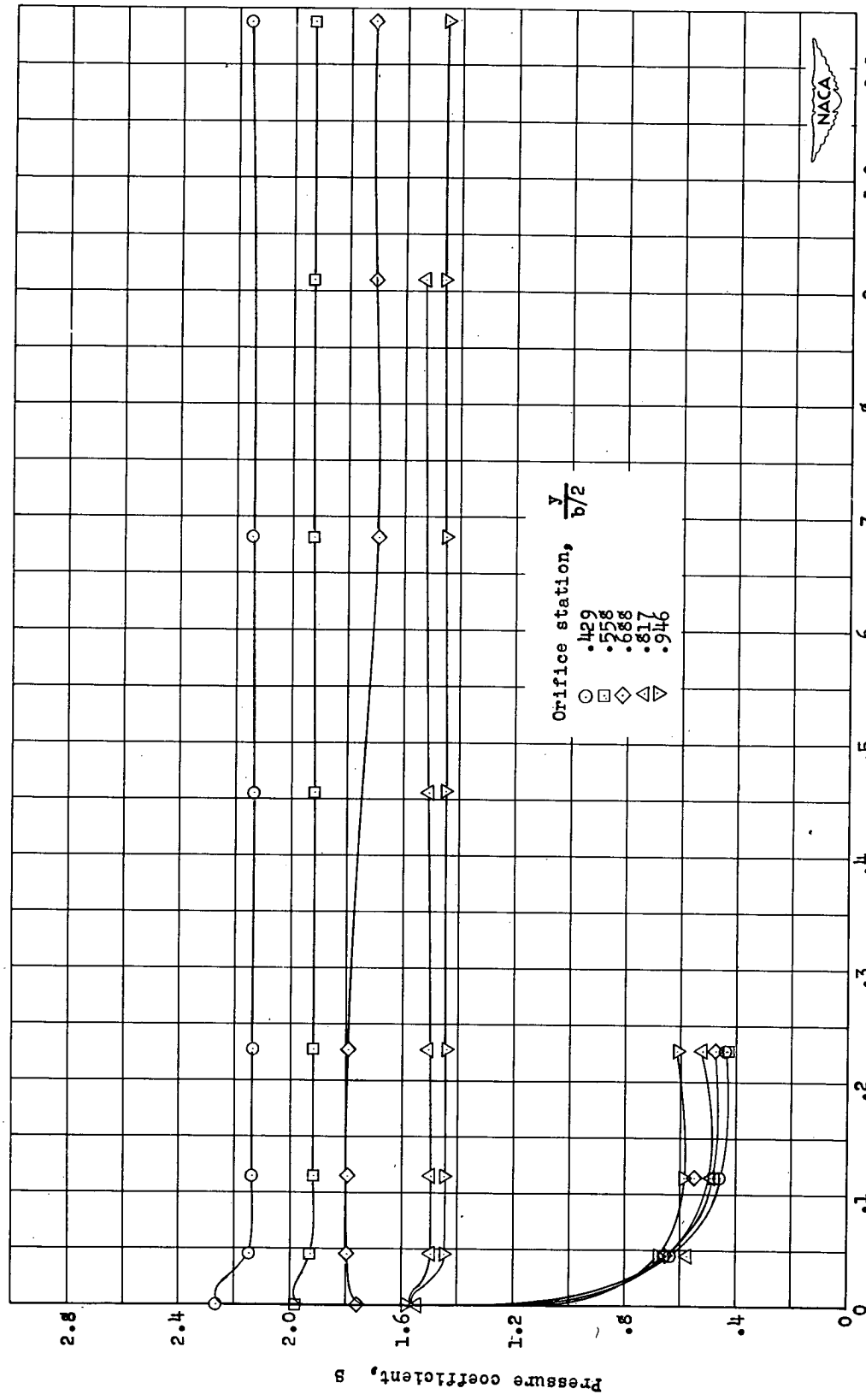

(c) $\alpha = 20.6°$.

Figure 5.- Concluded.

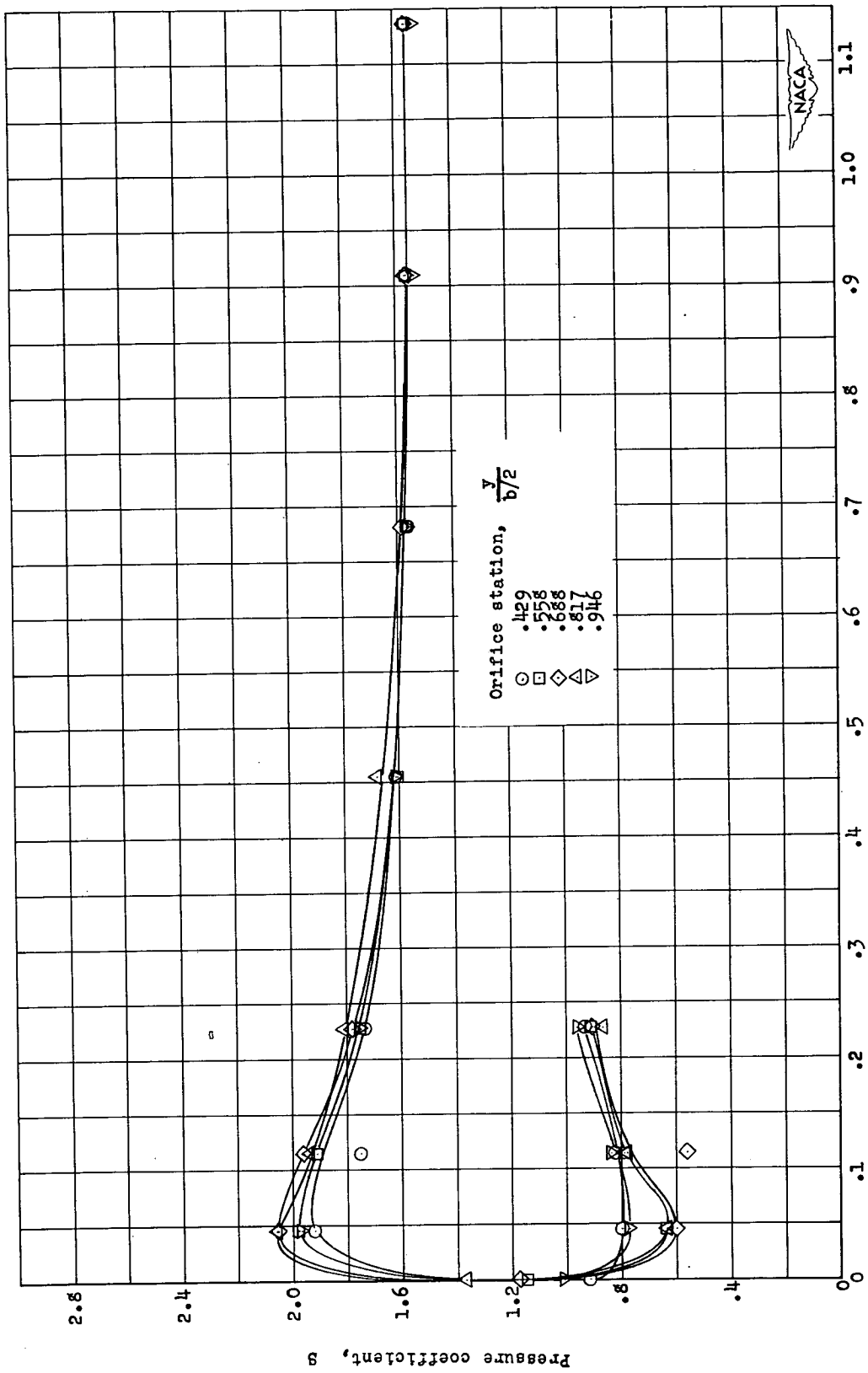

(a) $\alpha = 4.2°$.

Figure 6.- Pressure distribution about wing leading edge at various angles of attack. M = 0.60. Flap off.

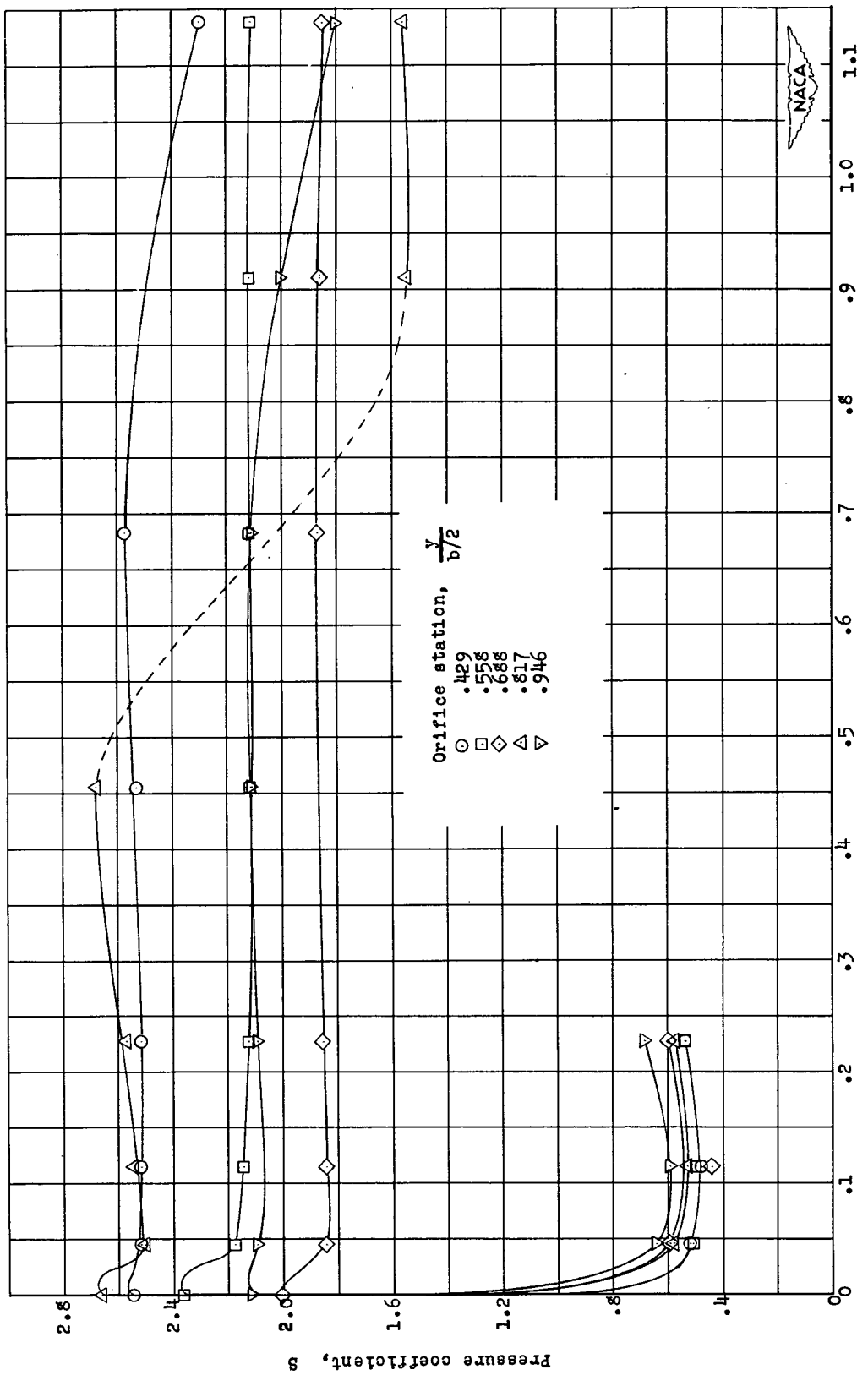

(b) $\alpha = 12.6^\circ$

Figure 6.- Continued.

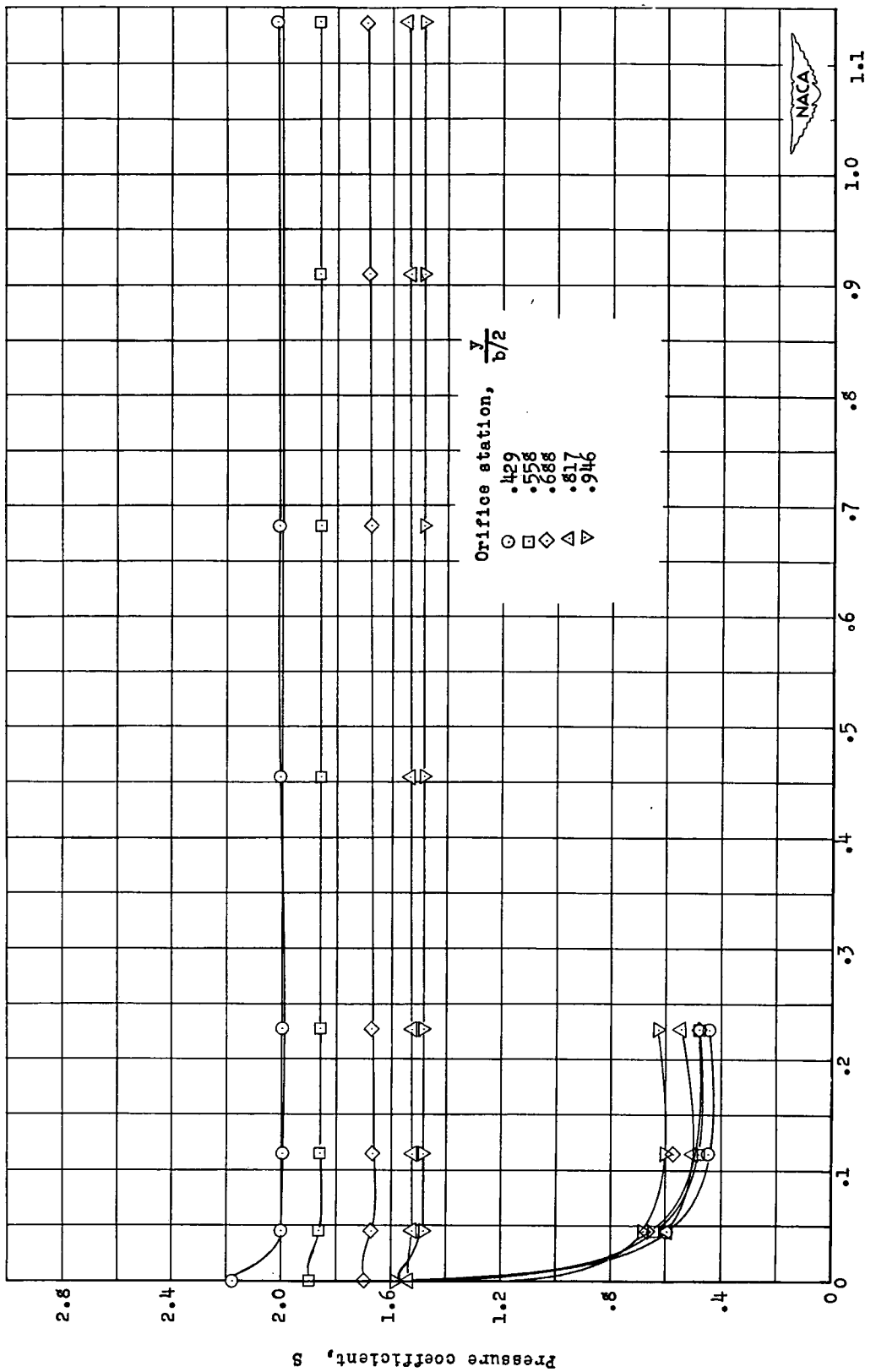

(a) $\alpha = 20.7°$.

Figure 6.- Concluded.

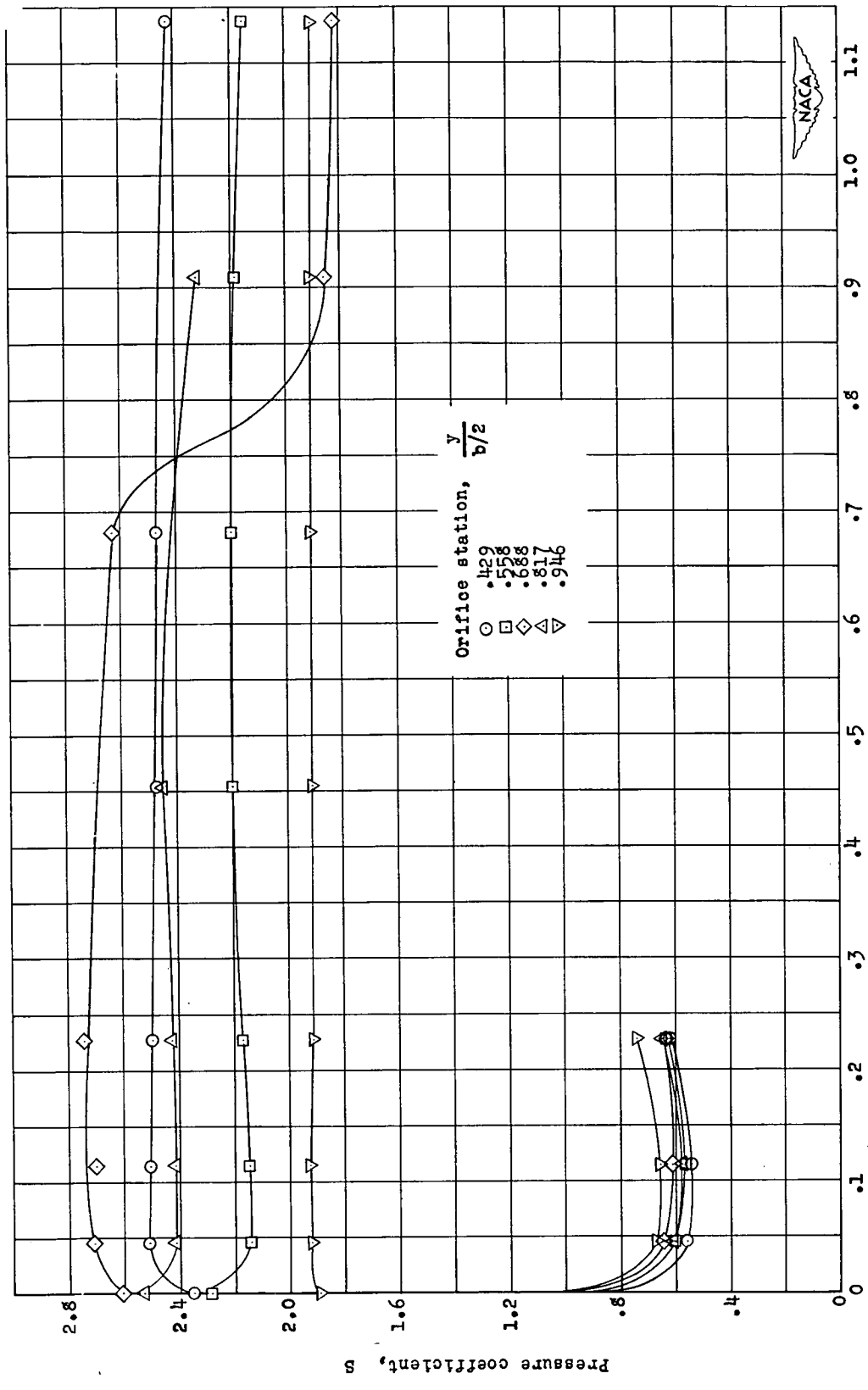

(a) $\alpha = 12.7°$.

Figure 7.- Pressure distribution about wing leading edge at various angles of attack. M = 0.70. Flap off.

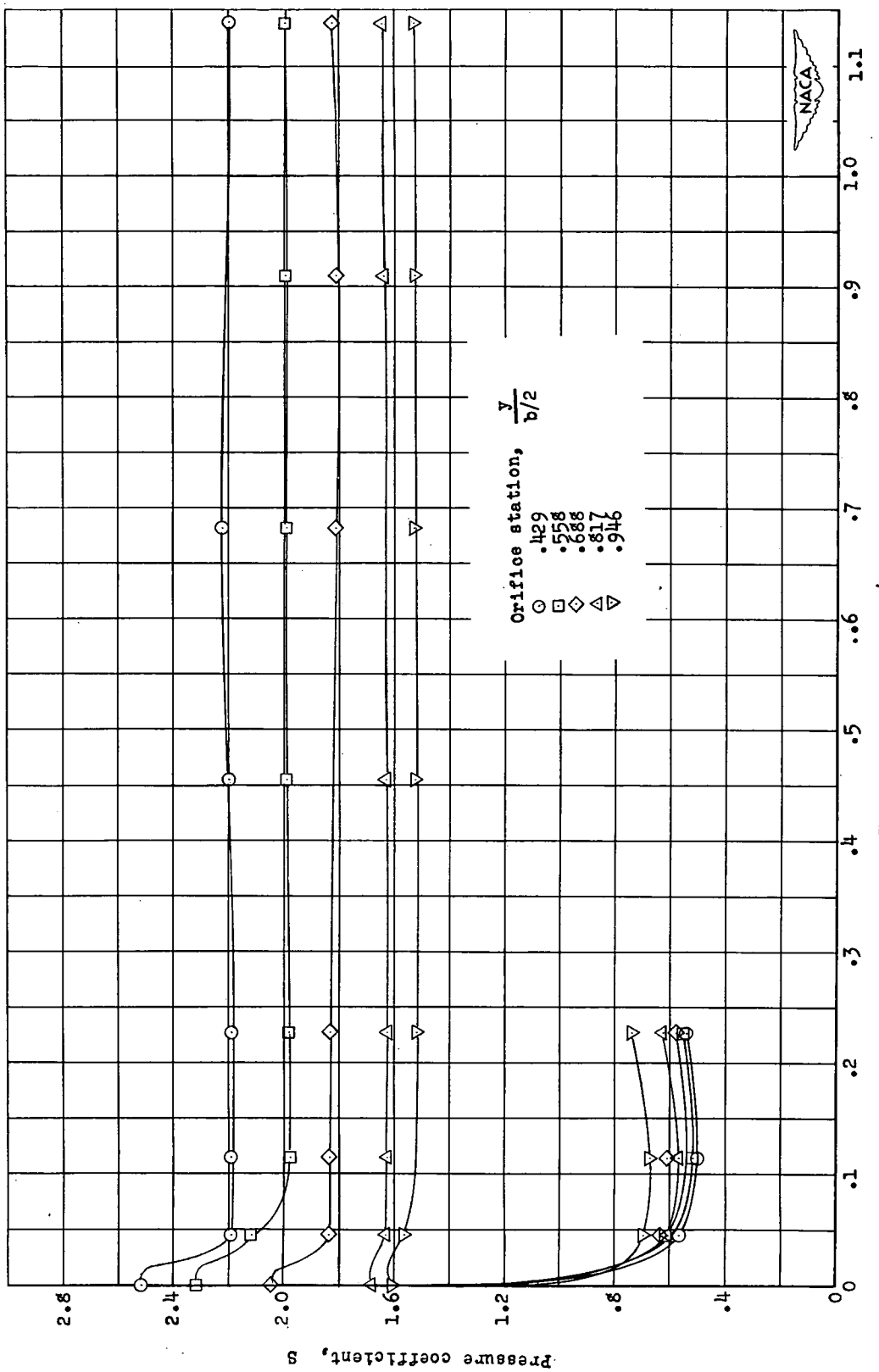

(b) $\alpha = 16.8°$.

Figure 7.- Continued.

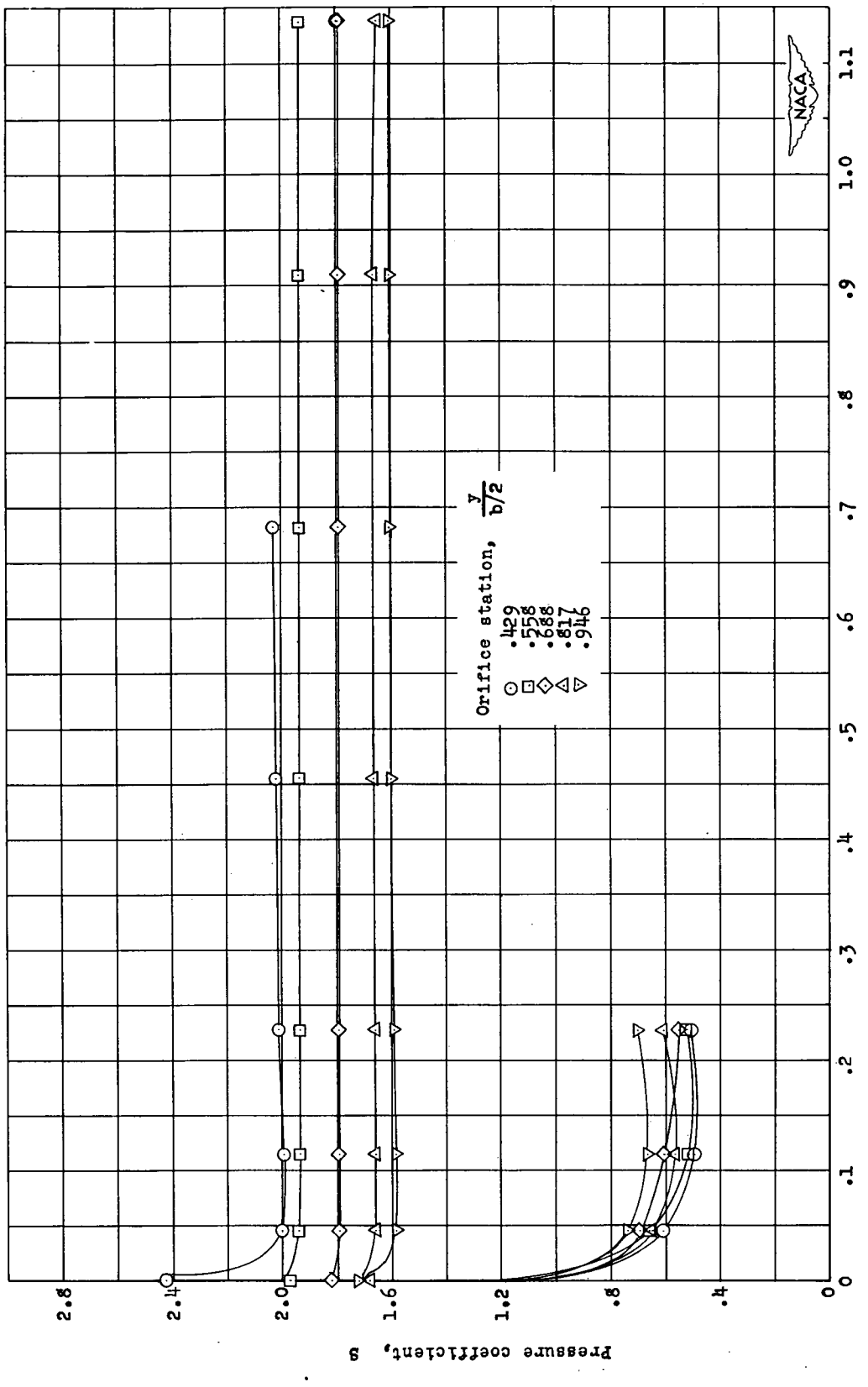

(c) $\alpha = 20.8°$.

Figure 7.- Concluded.

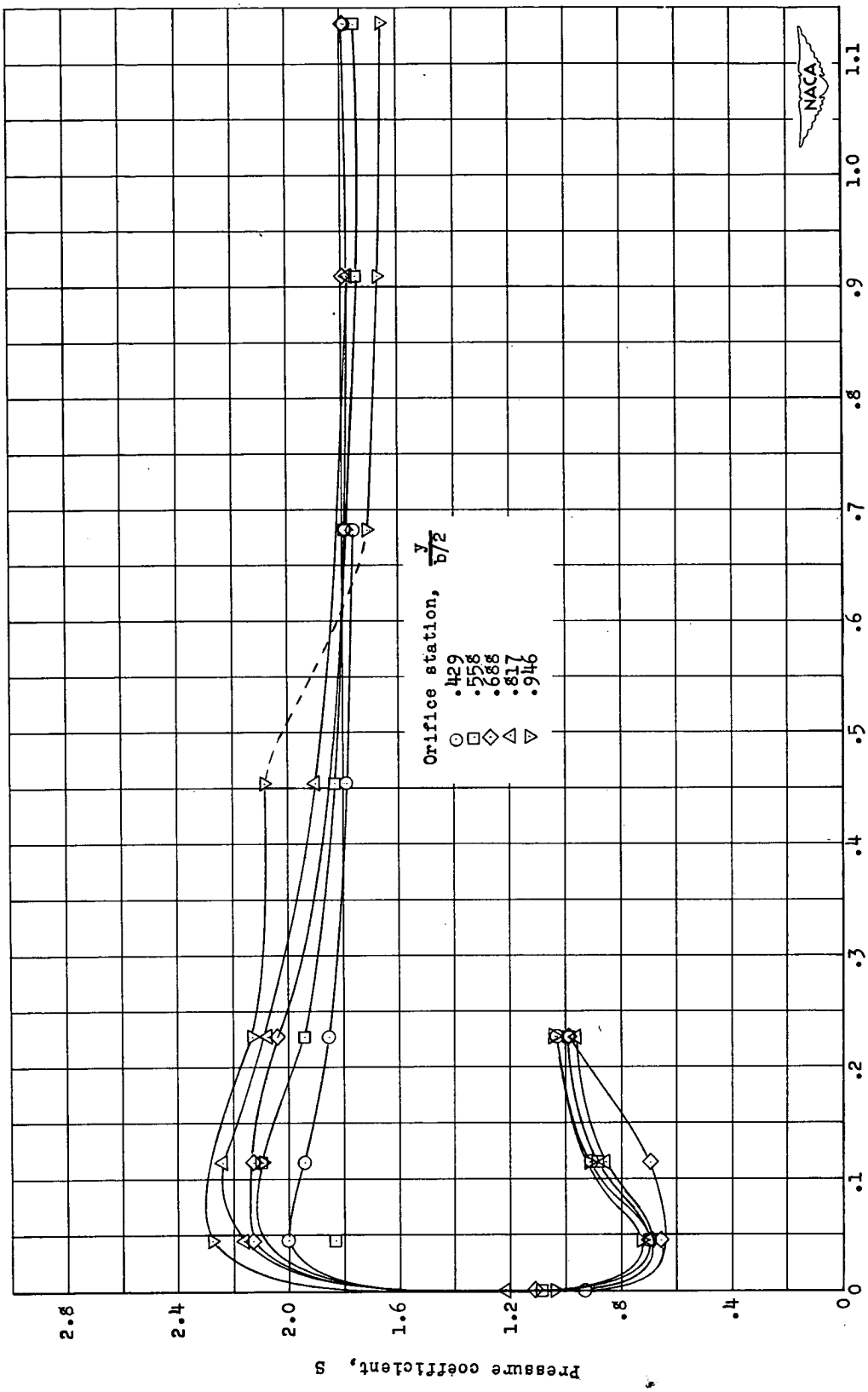

(a) $\alpha = 4.4°$.

Figure 8.- Pressure distribution about wing leading edge at various angles of attack. M = 0.80. Flap off.

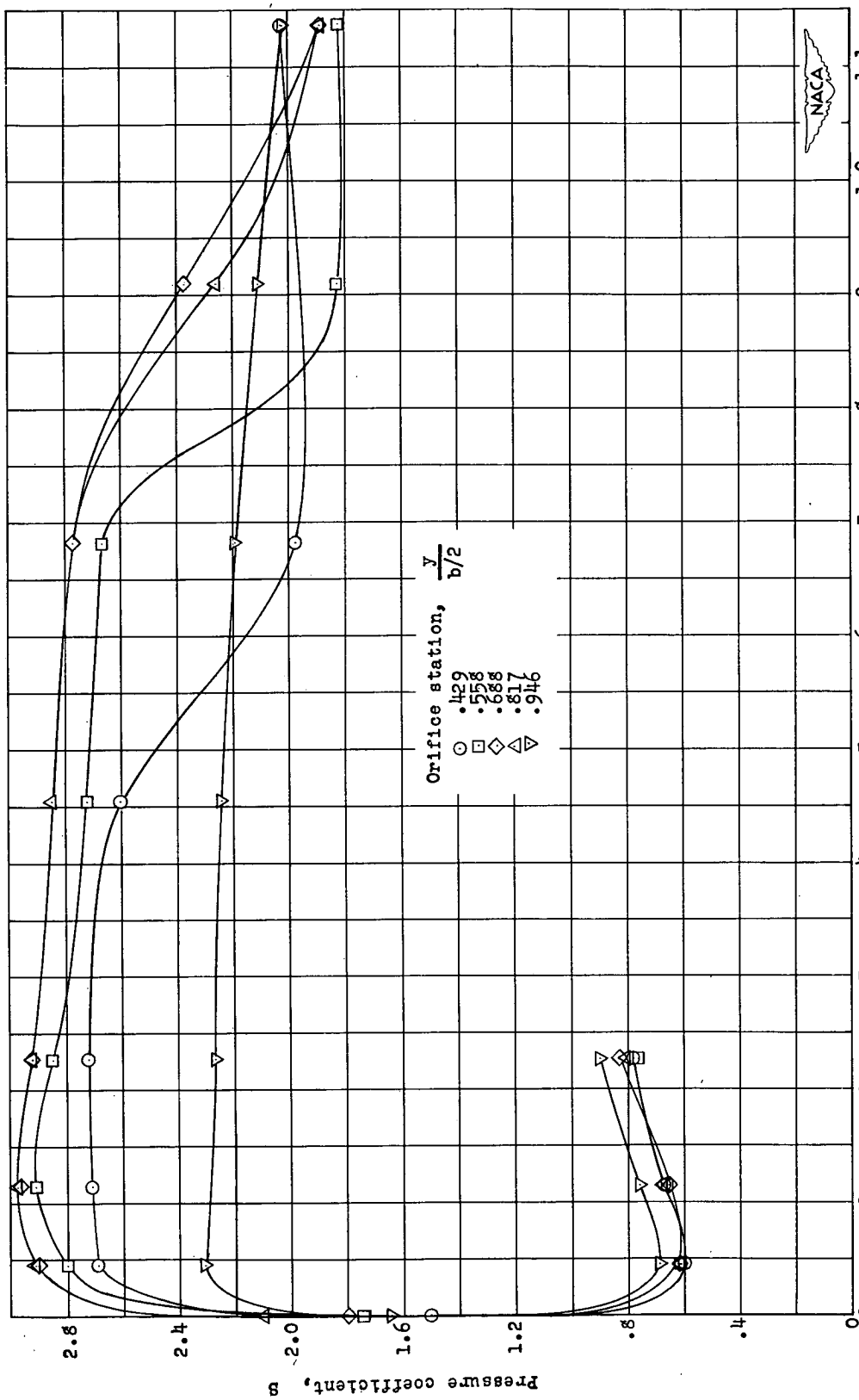

(b) $\alpha = 8.7^{\circ}$

Figure 8.- Continued.

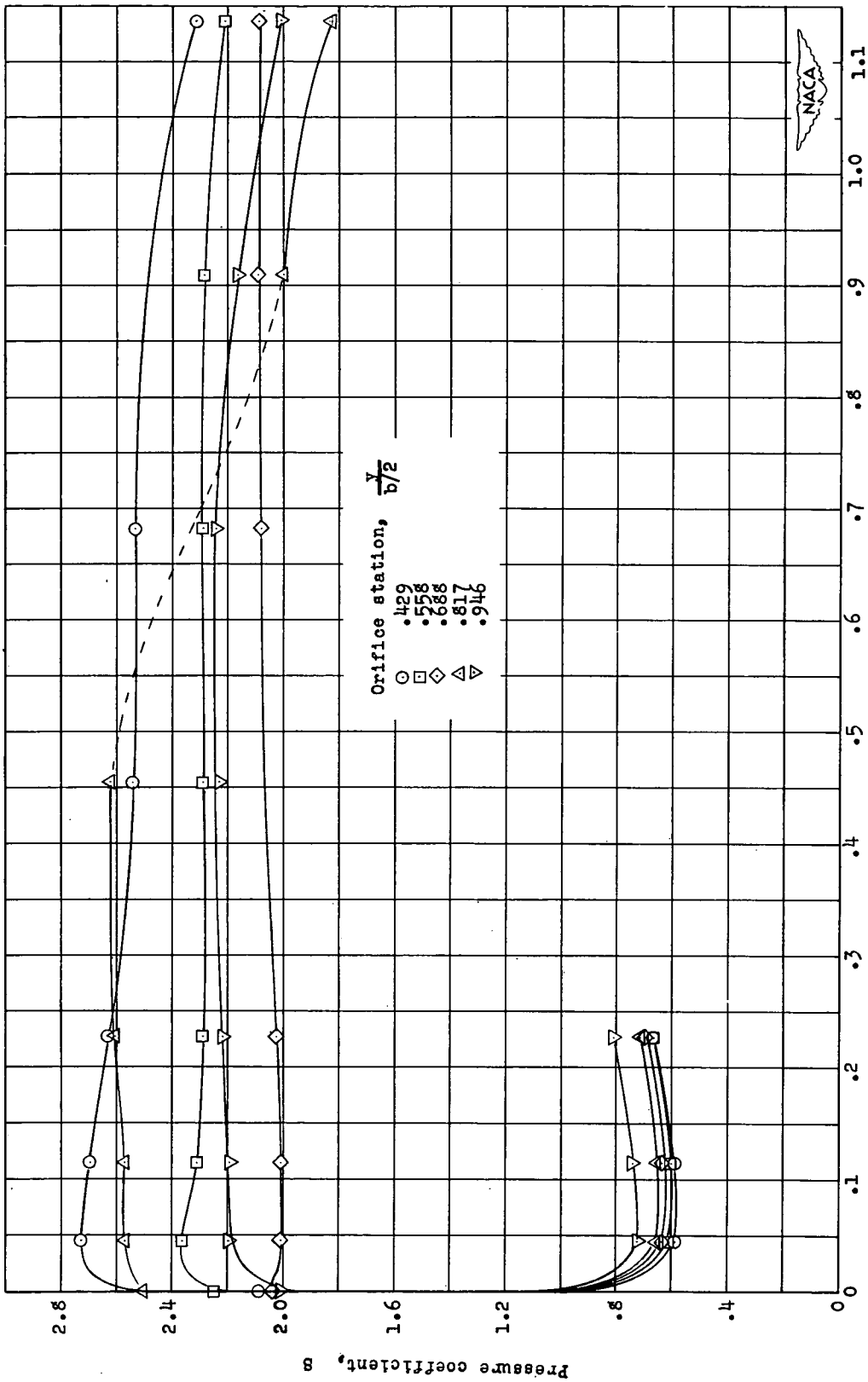

(c) $\alpha = 12.9°$.

Figure 8.- Continued.

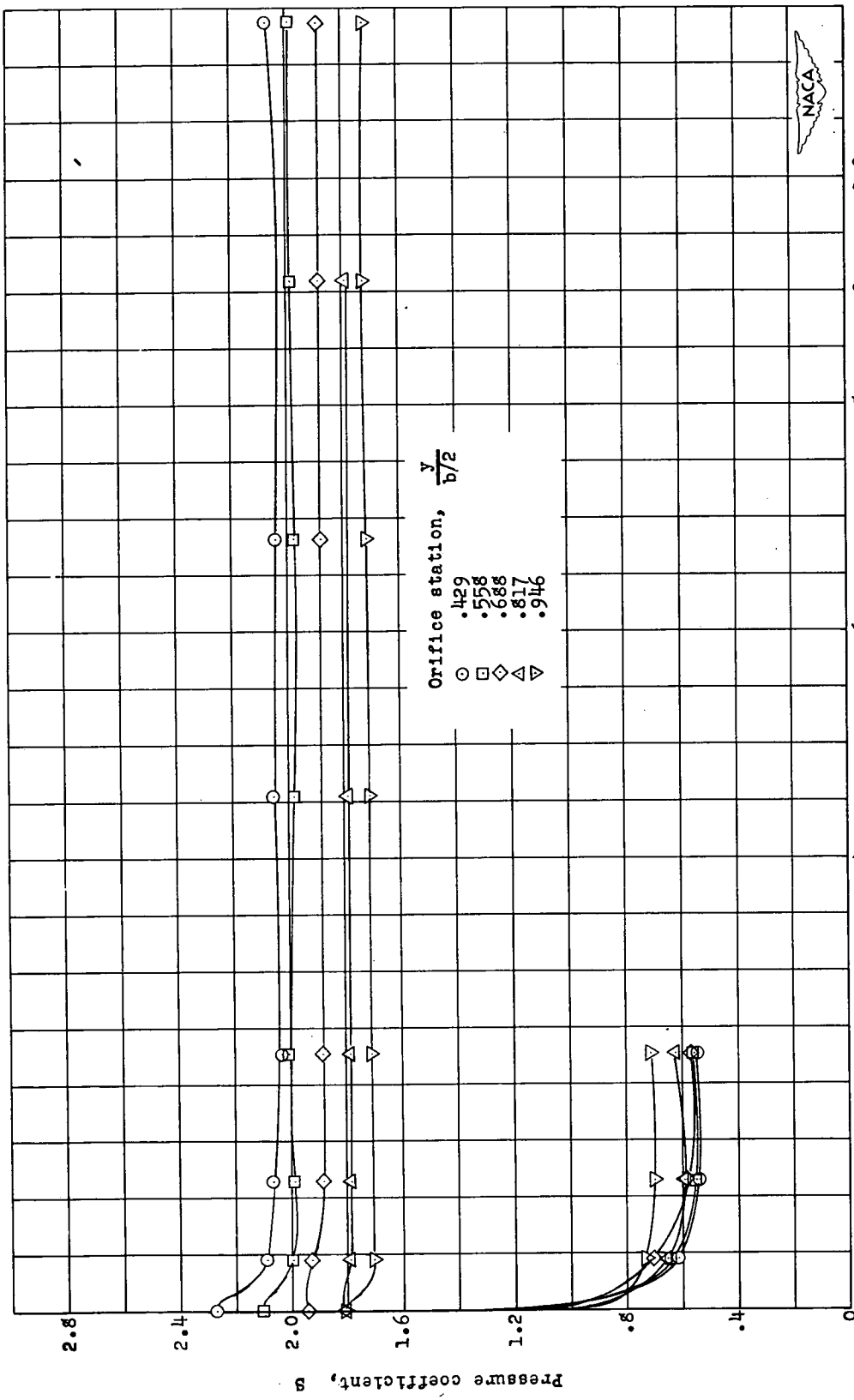

(d) $\alpha = 21.0^\circ$

Figure 8.- Concluded.

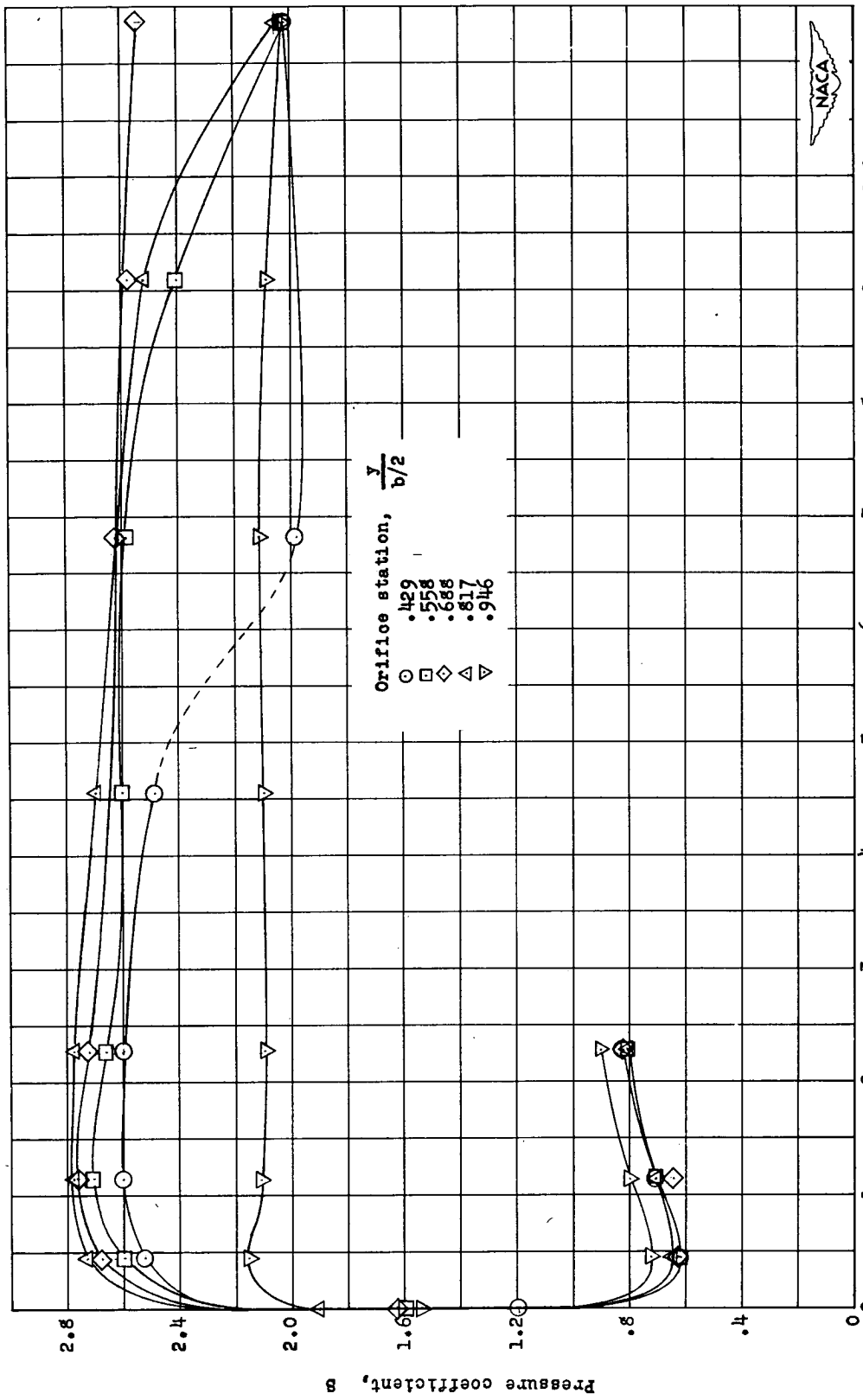

(a) $\alpha = 8.8^{\circ}$.

Figure 9.- Pressure distribution about wing leading edge at various angles of attack. M = 0.85. Flap off.

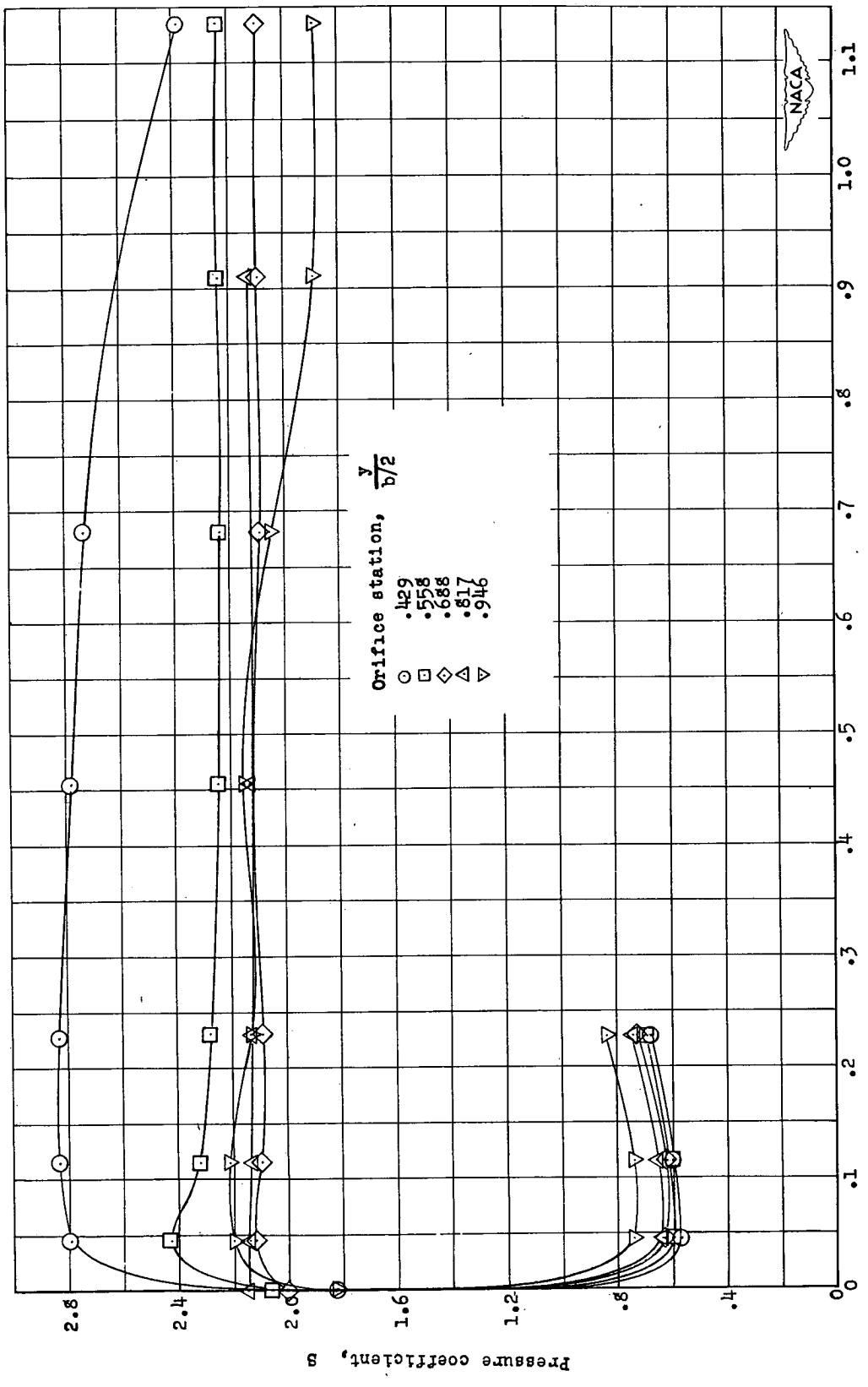

(b) $\alpha = 13.0°$.

Figure 9.- Continued.

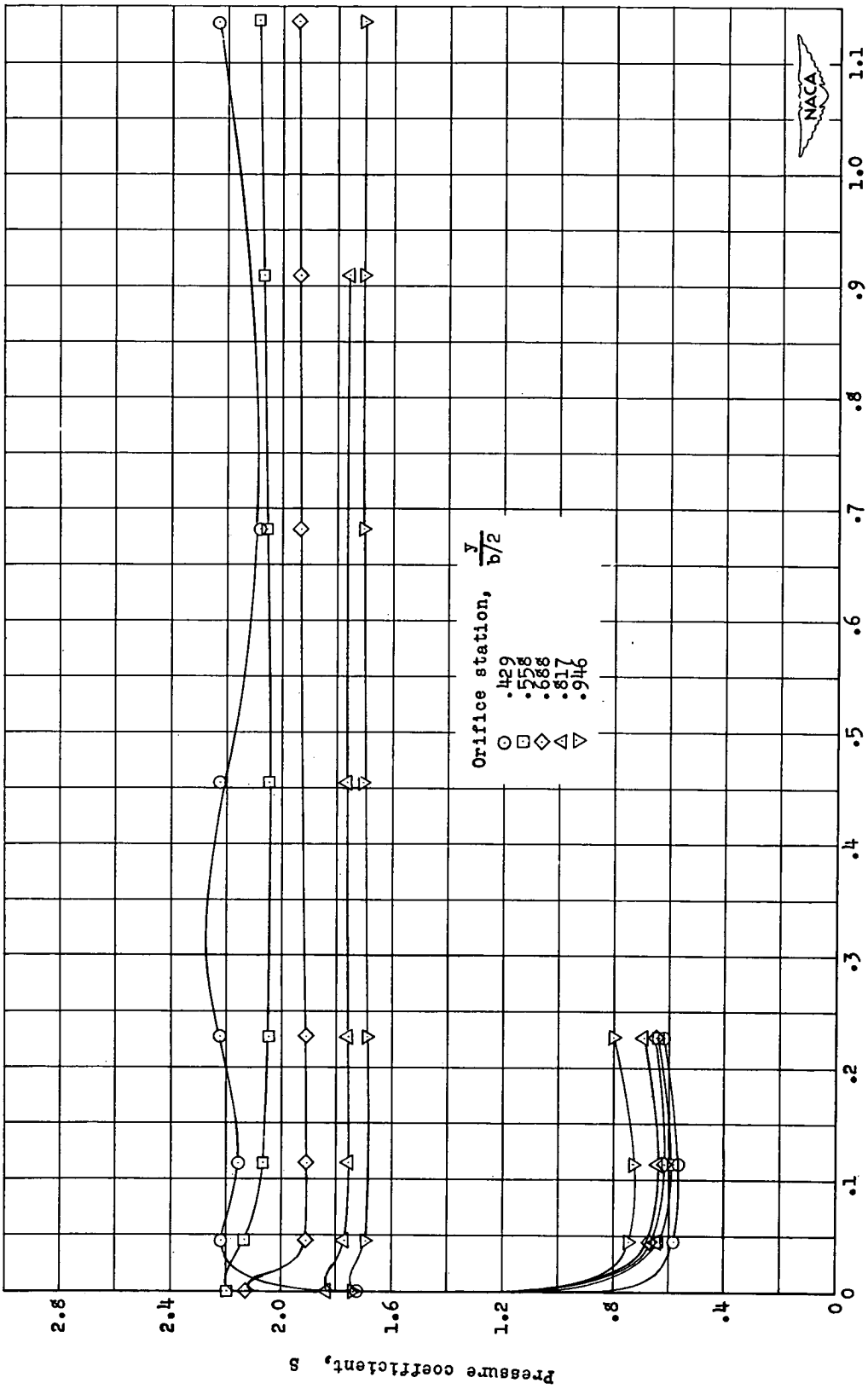

(c) $\alpha = 17.1^{\circ}$.

Figure 9.- Continued.

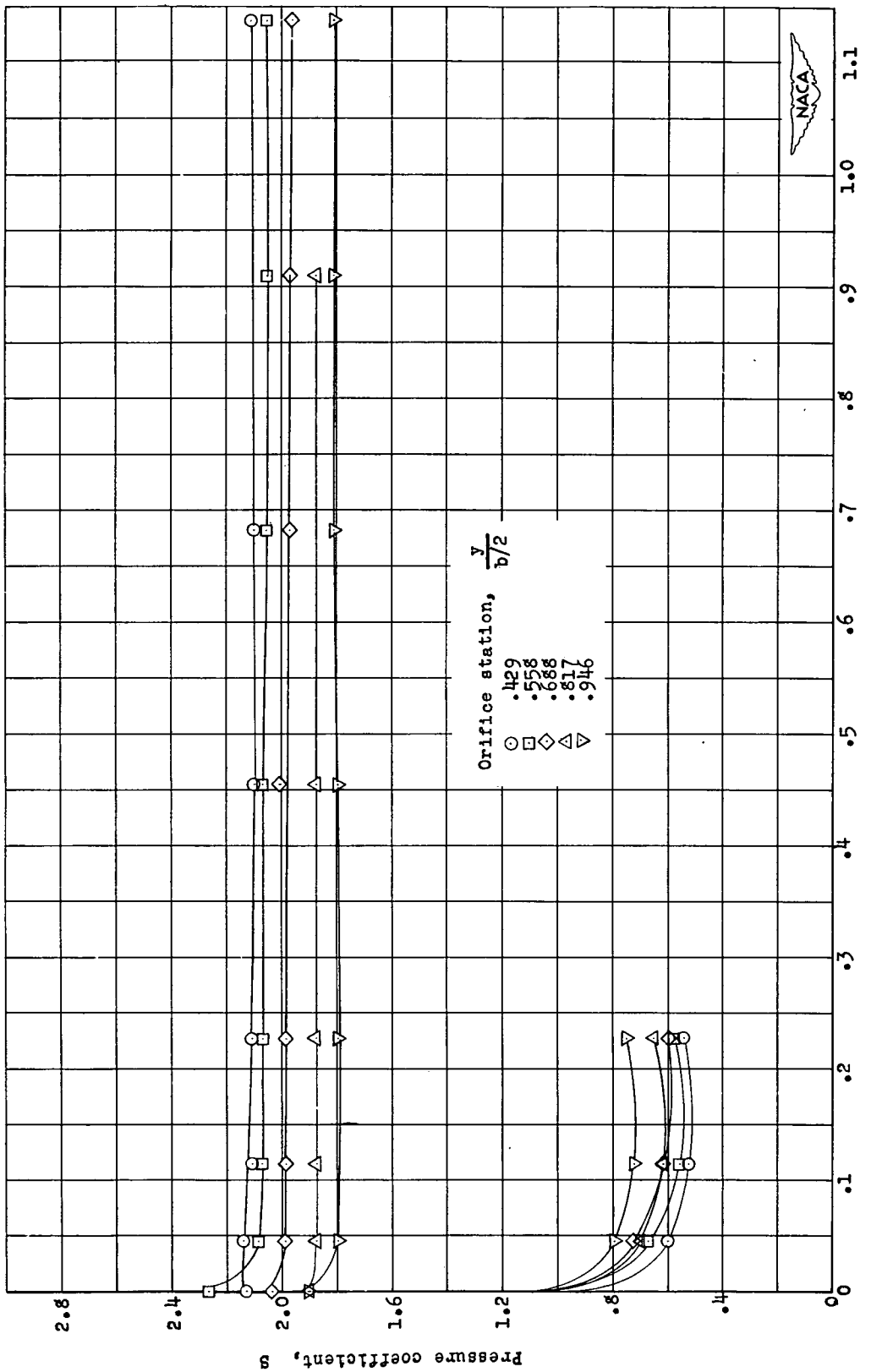

(d) $\alpha = 21.1^\circ$.

Figure 9.- Concluded.

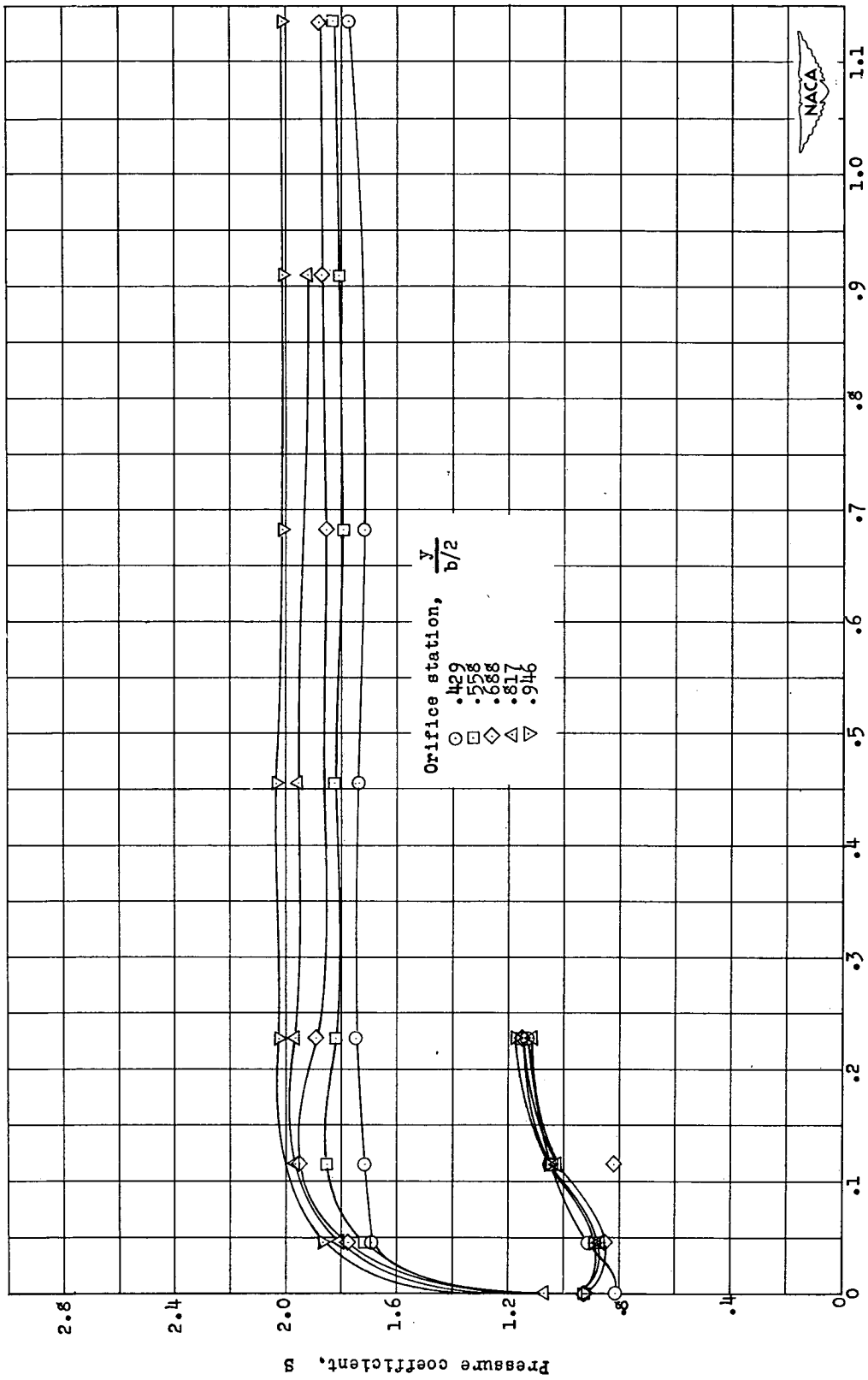

(a) $\alpha = 4.5°$.

Figure 10.- Pressure distribution about wing leading edge at various angles of attack. M = 0.90. Flap off.

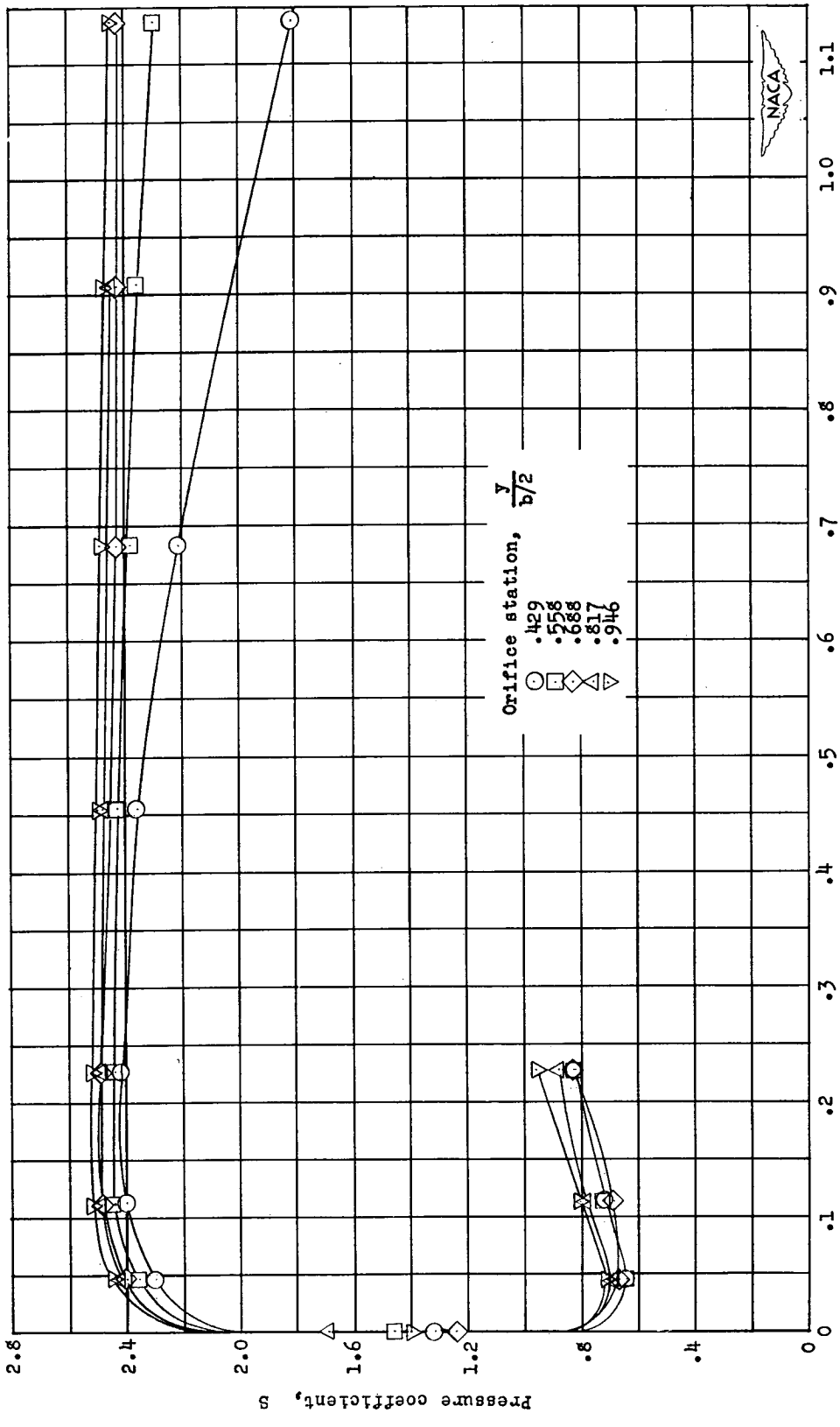

(b) $\alpha = 11.3°$.

Figure 10.- Concluded.